International Journal of
Molecular Sciences

MDPI

Review

Bioenergetics and Reactive Nitrogen Species in Bacteria

Vitaliy B. Borisov [1,*] and Elena Forte [2]

[1] Belozersky Institute of Physico-Chemical Biology, Lomonosov Moscow State University, Leninskie Gory, 119991 Moscow, Russia
[2] Department of Biochemical Sciences, Sapienza University of Rome, 00185 Rome, Italy; elena.forte@uniroma1.it
* Correspondence: viborborbor@yahoo.com

Abstract: The production of reactive nitrogen species (RNS) by the innate immune system is part of the host's defense against invading pathogenic bacteria. In this review, we summarize recent studies on the molecular basis of the effects of nitric oxide and peroxynitrite on microbial respiration and energy conservation. We discuss possible molecular mechanisms underlying RNS resistance in bacteria mediated by unique respiratory oxygen reductases, the mycobacterial *bcc-aa*$_3$ supercomplex, and *bd*-type cytochromes. A complete picture of the impact of RNS on microbial bioenergetics is not yet available. However, this research area is developing very rapidly, and the knowledge gained should help us develop new methods of treating infectious diseases.

Keywords: bacterial pathogen; host defense; infectious diseases; human health; molecular bioenergetics; electron transport chain; terminal oxidase; cytochrome oxidase; membrane protein

Citation: Borisov, V.B.; Forte, E. Bioenergetics and Reactive Nitrogen Species in Bacteria. *Int. J. Mol. Sci.* **2022**, *23*, 7321. https://doi.org/10.3390/ijms23137321

Academic Editor: Juan M. Tomás

Received: 8 June 2022
Accepted: 28 June 2022
Published: 30 June 2022

1. Introduction

Primary bacterial pathogens are infectious agents responsible for severe and often deadly diseases in humans. In addition, commensal bacteria can produce opportunistic infections in immunosuppressed patients. Disease-causing bacteria are becoming resistant to most commonly available antibiotics, which poses a threat to global public health. The production of reactive nitrogen species (RNS) by the innate immune system is part of the host's defense against invading microbes. RNS refers to various nitrogenous products including nitric oxide ($^{\bullet}NO$), peroxynitrite anion ($ONOO^-$), nitroxyl (HNO), dinitrogen trioxide (N_2O_3), nitrite (NO_2^-), nitrogen dioxide ($^{\bullet}NO_2$), nitronium cation (NO_2^+), nitrosonium cation (NO^+), nitrosoperoxycarbonate anion ($ONOOCO_2^-$), nitryl chloride ($Cl\text{-}NO_2$), S-nitrosothiols (RSNOs) [1]. $^{\bullet}NO$, along with carbon monoxide and hydrogen sulfide, is considered an endogenous gaseous signaling molecule [2–5]. $^{\bullet}NO$ is the main RNS produced by the host and the main source for the generation of the other RNS. This small diatomic molecule is a free radical, i.e., with one unpaired electron, and can diffuse easily through biological membranes. The enzymes that produce $^{\bullet}NO$ are NO synthases (NOS). They convert L-arginine and O_2 into L-citrulline and $^{\bullet}NO$ using NADPH as the electron donor. There are three NOS isoforms: neuronal (nNOS), endothelial (eNOS), and inducible (iNOS). nNOS and eNOS are constitutively expressed whereas iNOS expression is induced by immunological stimuli. The latter occurs predominantly in macrophages and plays an essential role in immune defense. $^{\bullet}NO$ can combine with superoxide radical ($O_2^{\bullet-}$) produced by the NADPH oxidase at diffusion-controlled rates yielding another RNS, $ONOO^-$. Under physiological conditions, $ONOO^-$ is in equilibrium with peroxynitrous acid, ONOOH (pK_a = 6.8), and local pH affects peroxynitrite reactivity. Both $ONOO^-$ and ONOOH are able to cross biological membranes. Peroxynitrite is a potent oxidant and nitrating agent, with a very important role in the destruction of invading pathogens by macrophages, as ONOOH spontaneously homolyzes to hydroxyl radical ($^{\bullet}OH$) and $^{\bullet}NO_2$ [6,7]. As they are within bacteria-containing phagolysosomes in macrophages, RNS creates a hostile

environment that impairs microbial growth. RNS inhibit DNA replication and bacterial respiration [8]. •NO and $ONOO^-$ were reported to damage metalloproteins containing heme cofactors and/or iron-sulfur clusters [9]. Additionally, •NO mediates post-translational modifications through S-nitrosylation of protein thiol groups, and peroxynitrite promotes the nitration of protein tyrosine residues [6,10]. This review focuses on the effects of •NO and $ONOO^-$ on bacterial aerobic (O_2-dependent) respiratory (electron transport) chains, namely on their last component represented by a heme-containing terminal oxidase, in light of recent findings.

We have chosen to focus only on aerobic bacteria because data on the RNS stress response of pathogenic anaerobes remain scarce. For instance, in the case of multidrug-resistant *Klebsiella pneumoniae*, a common cause of hospital-acquired pneumonia, some data on its adaptive response toward oxidative stress are available [11,12] but none addressed the bacterial response to •NO. A search of the genome of *K. pneumoniae* points out the presence of •NO-detoxifying enzymes Hmp and Hcp nonetheless [9]. The intracellular pathogen *Shigella flexneri*, which is the causative agent of bacillary dysentery, was reported to be sensitive to •NO produced *in vitro*; on the contrary, •NO is not required for clearance of the microbes in infected mice or macrophages [13]. A search of the genome of *S. flexneri*, however, indicates putative flavorubredoxin, Hmp and Hcp enzymes are involved in nitrosative detoxification [9]. *Clostridioides difficile* is the cause most implicated in antibiotic-associated diarrhea and severe inflammation of the bowel. This anaerobic enteropathogen encodes a few putative •NO-consuming enzymes, such as two flavodiiron proteins FdpA and FdpF, and Hcp [14,15]. FdpA and FdpF, however, show negligible •NO reductase activity but instead significant O_2 reductase activity [15,16]. Although there is no data on the specific •NO activity of Hcp, the physiological nitrosating agent S-nitrosoglutathione (GSNO) was reported to induce the expression of *hcp* [17]. This finding indicates that Hcp is involved in •NO resistance.

2. Bacterial Aerobic Respiratory Chains

Similar to mitochondria of eukaryotic cells, bacteria contain aerobic respiratory chains. The main function of the chains is to create a proton motive force (PMF), a central energy currency. The well-known mammalian mitochondrial chain is linear [18,19]. It consists of the enzyme complexes I, II, III, and IV (Table 1). The complexes I, III, and IV catalyze the oxidation of NADH by ubiquinone, oxidation of ubiquinol by ferricytochrome *c*, and oxidation of ferrocytochrome *c* by molecular oxygen, respectively. Each redox reaction is coupled to the generation of PMF that can be used further for the production of one more central energy currency, ATP, by ATP synthase (also termed complex V) or for active transport of solutes across the membrane. Complex II (succinate dehydrogenase) belongs to both the respiratory chain and the Krebs cycle. Complex II catalyzes the electron transfer from succinate to ubiquinone but unlike complexes I, III, and IV, the transfer is not coupled to the formation of PMF [20,21]. The bacterial respiratory chains, in contrast to the mitochondrial one, are branched, with different routes of electron transfer depending on the growth conditions [22,23]. As a quinone, bacteria can use not only ubiquinone but also menaquinone, plastoquinone, or caldariellaquinone.

Table 1. Major enzyme complexes of the mammalian mitochondrial electron transport chain.

Enzyme Complex	Electron Donor	Electron Acceptor	Energy Currency Produced
Complex I	NADH	ubiquinone	proton motive force (PMF)
Complex II	succinate	ubiquinone	none
Complex III	ubiquinol	ferricytochrome *c*	PMF
Complex IV	ferrocytochrome *c*	O_2	PMF

In order to transfer electrons from NADH to quinone, bacteria use three different families of NADH:quinone reductases (dehydrogenases)—NDH-1, NDH-2, and NQR (Table 2). NDH-1 reductases are closely related to the mitochondrial complex I and function as redox-driven proton pumps [24,25]. Both NDH-2 and NQR are unrelated to the canonical complex I. NDH-2 enzymes are non-electrogenic and therefore unable to support PMF [26,27]. NQR reductases operate as redox-driven sodium pumps, i.e., they generate a sodium ion motive force rather than PMF [28–30]. The sodium ion motive force, along with PMF and ATP, is the third energy currency used by a few bacteria [31]. Bacteria with more than one NADH:quinone reductase show a preference for one or another enzyme depending on the growth conditions.

Table 2. Major enzyme complexes found in aerobic bacterial electron transport chains.

Enzyme Complex	Electron Donor	Electron Acceptor	Energy Currency Produced
NDH-1	NADH	quinone	PMF
NDH-2	NADH	quinone	none
NQR	NADH	quinone	Na^+ motive force
Complex II	succinate	quinone	none
Complex III	quinol	ferricytochrome *c*	PMF
Heme–copper oxidases (aa_3, caa_3, bo_3, cbb_3, ba_3)	ferrocytochrome *c* or quinol	O_2	PMF
Cytochrome *bcc*-aa_3 supercomplex	quinol	O_2	PMF
Cytochrome *bd* (*bd*-I, *bd*-II)	quinol	O_2	PMF
Cyanide insensitive *bd*-type oxidase (CIO)	quinol	O_2	n.d.

Bacterial complex III, also termed cytochrome bc_1 complex, transfers electrons from quinol to ferricytochrome *c*. This redox reaction is coupled with the production of PMF via the Q-cycle (Mitchellian redox-loop) mechanism [32,33]. The presence of complex III in bacterial respiratory chains is optional. Some bacteria, e.g., *Escherichia coli*, have no cytochrome *c* at all, and hence no cytochrome bc_1 [34]. Cytochrome *c* of other bacteria is not water-soluble but fused either to complex III or complex IV. This leads to the formation of a supercomplex between complex III and complex IV (Table 2). Accordingly, the cytochrome *bcc*-aa_3 (III_2–IV_2) supercomplex was discovered in *Mycobacterium smegmatis* and *Corynebacterium glutamicum* [35–37]. A supercomplex composed of cytochrome bc_1 and aa_3-type cytochrome *c* oxidase was also identified in *Rhodobacter sphaeroides* [38]. Figure 1 shows examples of three different types of branched bacterial respiratory chains in which the complex III is absent (*E. coli* [34]), present as a separate enzyme (*Pseudomonas aeruginosa* [29]), or forms a tight supercomplex with the aa_3-type cytochrome *c* oxidase (*M. tuberculosis* [39,40]).

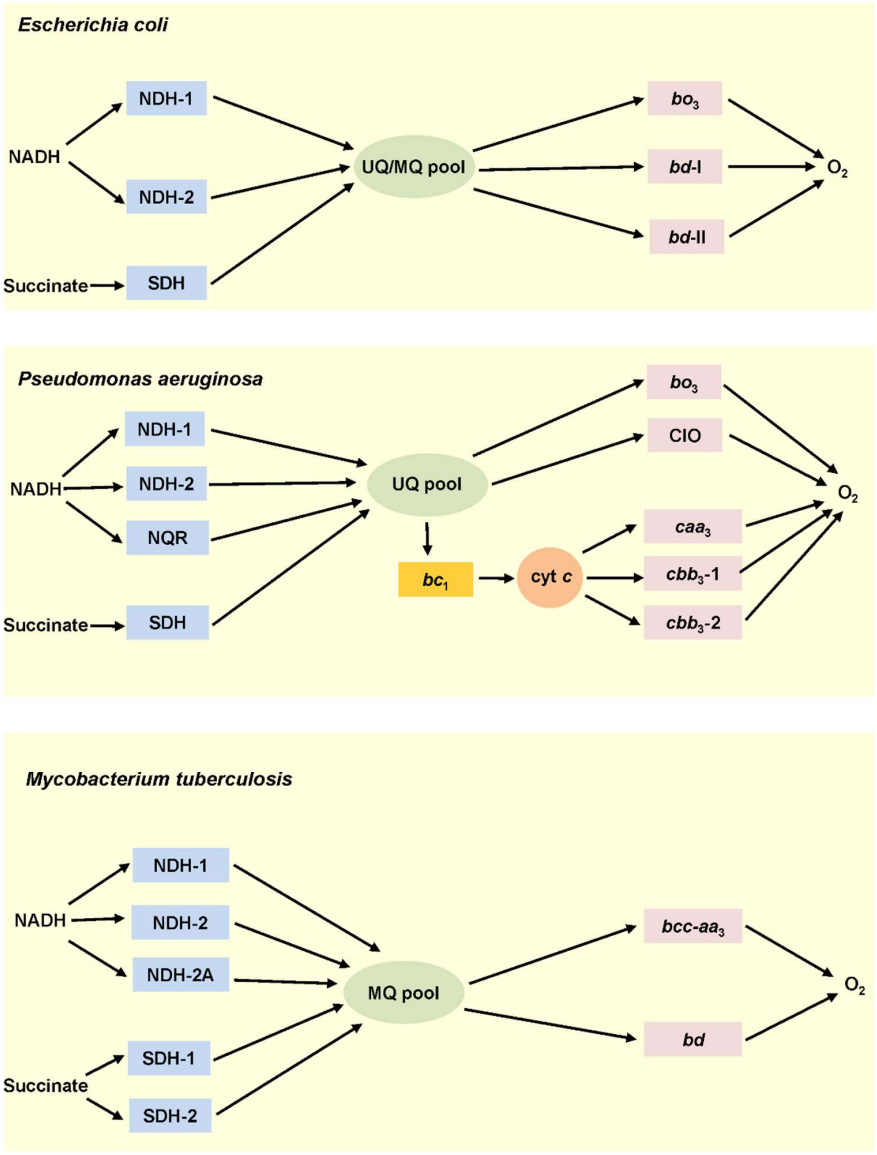

Figure 1. Aerobic respiratory chains of *Escherichia coli*, *Pseudomonas aeruginosa*, and *Mycobacterium tuberculosis*. In *E. coli*, two NADH dehydrogenases, NDH-1 and NDH-2, and succinate dehydrogenase (SDH) transfer electrons to ubiquinone (UQ)/menaquinone (MQ) pool. Three quinol oxidases, cytochromes bo_3, *bd*-I, and *bd*-II, oxidize ubiquinol/menaquinol with the concomitant reduction of O_2 to $2H_2O$. *P. aeruginosa* has three NADH dehydrogenases, NDH-1, NDH-2, NQR, and SDH. The electrons from ubiquinol are further transferred to O_2 either directly via two quinol oxidases, cytochrome bo_3 and *bd*-type cyanide insensitive oxidase (CIO), or via the bc_1 complex to three cytochrome *c* oxidases, caa_3, cbb_3-1, and cbb_3-2. *M. tuberculosis* possesses three NADH dehydrogenases, one NDH-1, two NDH-2, and two succinate dehydrogenases, SDH-1 and SDH-2. The electrons from menaquinol are then transferred to O_2 via cytochrome *bd* or cytochrome *bcc-aa*$_3$ supercomplex.

The membrane-bound terminal oxidases are divided into two superfamilies: heme–copper oxidases and *bd*-type cytochromes [41–43]. The active site of a heme–copper oxidase termed the binuclear center (BNC) is composed of a high-spin heme (a_3, o_3, or b_3) and a copper ion (Cu_B). The enzyme catalyzes the transfer of electrons from cytochrome *c* or quinol to O_2 with the production of $2H_2O$. The reaction is coupled to the generation of PMF using the mechanism of redox-coupled proton pumping across the membrane [21,22,44–59]. A heme–copper oxidase that uses cytochrome *c* as an electron donor (cytochrome *c* oxidase) has the second copper site, Cu_A. Cu_A directly accepts electrons from cytochrome *c*. If the

enzyme uses quinol as an electron donor (quinol oxidase), Cu_A is absent. Heme–copper oxidases also contain a low-spin heme (*a* or *b*) that accepts electrons from Cu_A (cytochrome *c* oxidase) or directly from an electron donor (quinol oxidase) and donates them to the BNC. In caa_3 and cbb_3 oxidases, the reduction of Cu_A by water-soluble cytochrome *c* is followed by an intermediate reduction of additional heme(s) *c*. The classification of the heme–copper oxidases is based on the organization of the intraprotein proton transfer pathways. Accordingly, the enzymes are divided into three main families: A, B, and C [60–62].

The active site of cytochrome *bd* contains a high-spin heme *d* but not a copper ion [39,63–69]. There are data that one more high-spin heme, b_{595}, could perform some of the functions of Cu_B [70–86]. Similar to heme–copper oxidases, *bd*-type cytochromes couple the reduction of O_2 to $2H_2O$ to the formation of PMF [44,87,88]. However, in contrast to the heme–copper enzymes, cytochromes *bd* do so without being a proton pump [89–91]. The lack of proton-pumping machinery decreases the energetic efficiency of the *bd*-type oxidases. Until now, all biochemically characterized cytochromes *bd* turned out to be quinol oxidases [49,92–94]. Accordingly, the third heme in cytochrome *bd*, a low-spin b_{558}, mediates electron transfer from quinol to hemes b_{595} and *d*. The *bd*-oxidases typically have a very high affinity for O_2 and CO due to specific features of heme *d*, which is an iron-chlorin [77,95–99]. In some cases, heme *d* can be replaced with heme *b* [42,100]. Intriguingly, phylogenomic analyses performed by Murali et al. suggest that there are *bd*-type cytochromes that use cytochrome *c* as an electron donor [42]. Phylogenomics by Murali et al. identified three families and several subfamilies within the cytochrome *bd* superfamily. At the same time, earlier classification of the *bd*-type oxidases based on the size of the hydrophilic region between transmembrane helices 6 and 7 in subunit I (a binding domain for quinol oxidation termed the Q-loop) is still commonly used. According to this classification, cytochromes *bd* are divided into two subfamilies: L (long Q-loop) and S (short Q-loop) [101,102].

The catalytic cycle of heme–copper oxidases is best studied for the aa_3-type cytochrome *c* oxidases (Figure 2). It includes the intermediates termed O, E, R, A, P, F (see [41] and references therein). The sequential transfer of two electrons to O (the fully oxidized state of the BNC) results in the sequential formation of E and R, one-electron reduced and fully reduced states of the BNC, respectively. R binds O_2 to produce the A state. Then, the O–O bond is cleaved, and the P state is formed in which heme a_3 is ferryl, Cu_B is oxidized, and a conserved tyrosine residue in the BNC is oxidized to a radical, $Y^{\bullet}$. The transfer of the third electron to the BNC re-reduces $Y^{\bullet}$ to Y bringing about the F state. The transfer of the fourth electron to the BNC leads to the reduction of ferryl heme a_3 to ferric form that regenerates the O state and completes the cycle. The O→ E, E→ A, P→ F, and F→ O transitions are electrogenic and coupled to the transfer of a pumped proton (not shown in Figure 2).

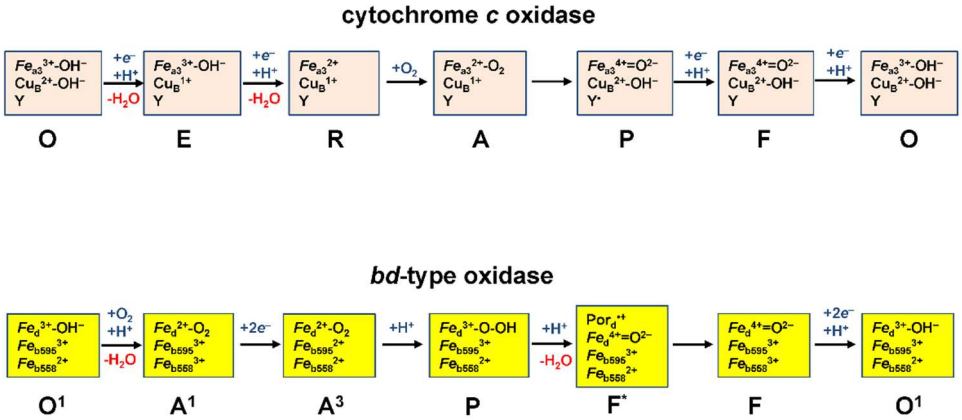

Figure 2. Proposed catalytic cycles of heme–copper cytochrome *c* oxidase and *bd*-type oxidase.

The catalytic cycle of *bd*-type oxidases is deduced from the studies on the *E. coli* cytochrome *bd*-I [90,103–106] (Figure 2). It includes the intermediates termed O^1, A^1, A^3, P,

F*, F, and takes into account that the quinol substrate is a two-electron donor. In the $O^1 \rightarrow A^1$ transition, an electron transfers from heme b_{558} to heme *d* and the latter binds O_2. In the next $A^1 \rightarrow A^3$ transition, two electrons from a quinol reduce heme b_{558} and heme b_{595}. In the $A^3 \rightarrow$ P transition, a true transient peroxy complex of ferric heme *d* is formed concomitant with oxidation of heme b_{595}. The O–O bond cleavage occurs in the next, P→ F* transition in which the ferric heme *d* is further oxidized to the ferryl form with a porphyrin π-cation radical ($Por^{\bullet+}$). Then in the F*→ F transition, the radical is quenched by an electron from the ferrous heme b_{558}. The F→ O^1 transition, in which two electrons from a second quinol reduce the ferryl heme *d* (to the ferric form) and heme b_{558}, completes the cycle. The P/F*→ F and F→ O^1 transitions were reported to be electrogenic [88–91,107].

The key role of most heme–copper oxidases in bacterial metabolism is to create PMF. In the case of cytochromes *bd*, the bioenergetic function is not the only. The *bd* enzymes play other critical roles in microbes [94,108–111]. They contribute significantly to the ability of bacteria to resist stresses induced by peroxide [49,112–116], sulfide [5,117–120], ammonia [121], chromate [122], cyanide [117,123]. Due to the fact that the *bd* oxidases are often found in pathogenic bacteria but absent in humans, they can be used as protein targets for next-generation antimicrobials [43,64,68,124–134].

3. •NO and Bacterial Terminal Oxidases

3.1. •NO and Bacterial Heme–Copper Terminal Oxidases

With the exception of the mycobacterial aa_3-type oxidase (see Section 3.1.1), the bacterial heme–copper oxidases tested to date, such as the cbb_3-type oxidases from *Vibrio cholerae* and *Rhodobacter sphaeroides*, and the aa_3-type oxidase from *R. sphaeroides*, are rapidly and strongly inhibited by •NO [135], similar to their mitochondrial homolog, cytochrome *c* oxidase [136]. The reaction of the mitochondrial enzyme with •NO was studied in more detail. It was shown that low, nanomolar levels of •NO reversibly inhibit the enzyme activity [136] whereas high, micromolar levels of •NO cause irreversible damage to the enzyme [137]. The reversible inhibition occurs via two pathways. At high reductive pressure (high turnover conditions) and low O_2 tensions, the O_2-competitive inhibition pathway prevails. It occurs through the reaction of •NO with the two-electron reduced (and possibly one-electron reduced) BNC leading to the production of the nitrosyl derivative of the enzyme. At low reductive pressure (low turnover conditions) and high O_2 tensions, the noncompetitive pathway prevails. The latter proceeds via reaction of •NO with the catalytic intermediates that have Cu_B oxidized, resulting in the generation of the nitrite-bound enzyme [138–141]. It is reasonable to assume that the bacterial heme–copper oxidases studied [135] are inhibited by •NO through similar mechanisms.

3.1.1. •NO-Metabolizing Activity of the Mycobacterial *bcc-aa*$_3$ Supercomplex in Turnover

Mycobacteria contain no water-soluble cytochrome *c*. Probably for this reason their aa_3-type cytochrome oxidase needs to be in a tight supercomplex with cytochrome *bcc*, a homolog of the mitochondrial cytochrome bc_1 [35,36]. Forte et al. reported that a purified chimeric supercomplex composed of *M. tuberculosis* cytochrome *bcc* and *M. smegmatis* aa_3-type oxidase resists inhibition by •NO [57]. The effect of •NO on the O_2 consumption by the *bcc-aa*$_3$ supercomplex in the presence of excess dithiothreitol (DTT) and menadione (MD) was evaluated amperometrically. A very small, short-term decrease in the O_2 consumption induced by •NO is followed by quick and complete restoration of the initial enzyme's activity (Figure 3, *inset*). Surprisingly, the •NO decay allowing for the activity recovery occurs much faster than one would expect. The reason for this turned out to be the ability of the *bcc-aa*$_3$ supercomplex to degrade •NO under turnover conditions. The rate of •NO decay in the presence of the enzyme and reductants is significantly higher than in the presence of the reductants only (Figure 3, *top panel*). Furthermore, in the absence of DTT and MD, the kinetic profiles of •NO decay in aerobic solution with and without the *bcc-aa*$_3$ are identical (Figure 3, *bottom panel*). The latter two observations support the conclusion that the •NO decomposition is indeed catalyzed by the purified *bcc-aa*$_3$ supercomplex in

turnover with O_2 and the electron donors. The maximum •NO-consuming activity of the enzyme measured following the addition of 30 μM •NO appeared to be about 300 mol •NO × (mol *bcc-aa*$_3$)$^{-1}$ × min^{-1} [57] (Table 3).

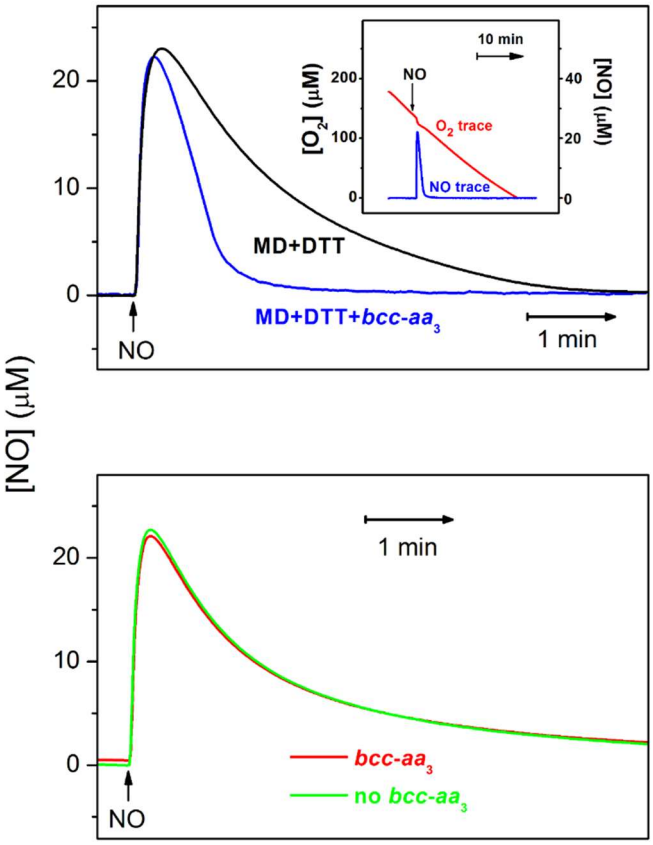

Figure 3. Purified mycobacterial cytochrome *bcc-aa*$_3$ supercomplex scavenges •NO under turnover conditions. ***Top panel:*** the *bcc-aa*$_3$ in turnover with 5 mM DTT and 0.26 mM MD accelerates the decomposition of 30 μM •NO added. (***Bottom panel)*** in the absence of DTT and MD, i.e., under non-turnover conditions, the *bcc-aa*$_3$ does not accelerate the decomposition of 30 μM •NO added. (***Inset***) the effect of 30 μM •NO on the O_2 consumption by the *bcc-aa*$_3$. The Figure was modified from Forte et al. [57] under the terms of the Creative Commons Attribution 4.0 International License.

Table 3. Overview of •NO interactions with mycobacterial cytochrome *bcc-aa*$_3$ supercomplex and *E. coli* cytochrome *bd*-I, respiratory enzyme complexes which contribute to mechanisms of bacterial resistance to •NO.

Enzyme Complex	Inhibition by •NO	•NO Degradation in Turnover	Anaerobic •NO Degradation	•NO off-Rate	NO_2^- off-Rate	Reference
Mycobacterial cytochrome *bcc-aa*$_3$ supercomplex	No	Yes (~300 mol •NO × (mol *bcc-aa*$_3$)$^{-1}$ × min^{-1})	Yes (~3 mol •NO × (mol *bcc-aa*$_3$)$^{-1}$ × min^{-1})	n.d.	n.d.	[57]
E. coli cytochrome *bd*-I	Yes (IC_{50} = 100 nM •NO at 70 μM O_2)	No	No	0.133 s^{-1}	n.d.	[142,143]

Possible mechanisms for this reaction catalyzed by the *bcc-aa*$_3$ are worth discussing. Earlier, it was reported that in the mitochondrial cytochrome oxidase, •NO can react with the catalytic intermediates O, P, and F, each according to a 1:1 stoichiometry [138,140]. One could suggest that in the *bcc-aa*$_3$ •NO also reacts with these species populated at a steady-state. In view of the fact that in the *bcc-aa*$_3$ the •NO/O_2 stoichiometry was estimated to be 2.65 [57] i.e., >1, we assume that in this enzyme •NO can react with more than one intermediate during the catalytic cycle. Figure 4 shows possible reaction pathways for the

bcc-aa$_3$ taking into account modern views on the structures of intermediates O, F, and P. As in the mitochondrial enzyme [138,140], in the reactions with O, F, and P, •NO is thought to donate one electron to Cu_B^{2+} yielding nitrosonium ion (NO^+) and Cu_B^{1+}. This results in the oxidation of •NO to NO_2^- and the conversion of a corresponding intermediate into the succeeding one along the catalytic cycle of the *bcc-aa*$_3$ (Figure 4, reactions 1, 2, 3, see also Figure 2). In other words, following the reaction with one molecule of •NO, O is converted into E, F—into O, and P—into F. In the mitochondrial cytochrome oxidase, NO_2^- produced from •NO binds with a relatively high affinity to the oxidized heme a_3 (or Cu_B) in the BNC [140]. This impedes the complete reduction of the BNC and, hence, its ability to bind and further reduce O_2. As a result, O_2 consumption is halted. We hypothesize that in the case of the *bcc-aa*$_3$ NO_2^- generated from •NO does not bind to the BNC with high affinity. Instead, NO_2^- is quickly ejected into the bulk phase from the supercomplex without affecting the catalytic O_2 consumption.

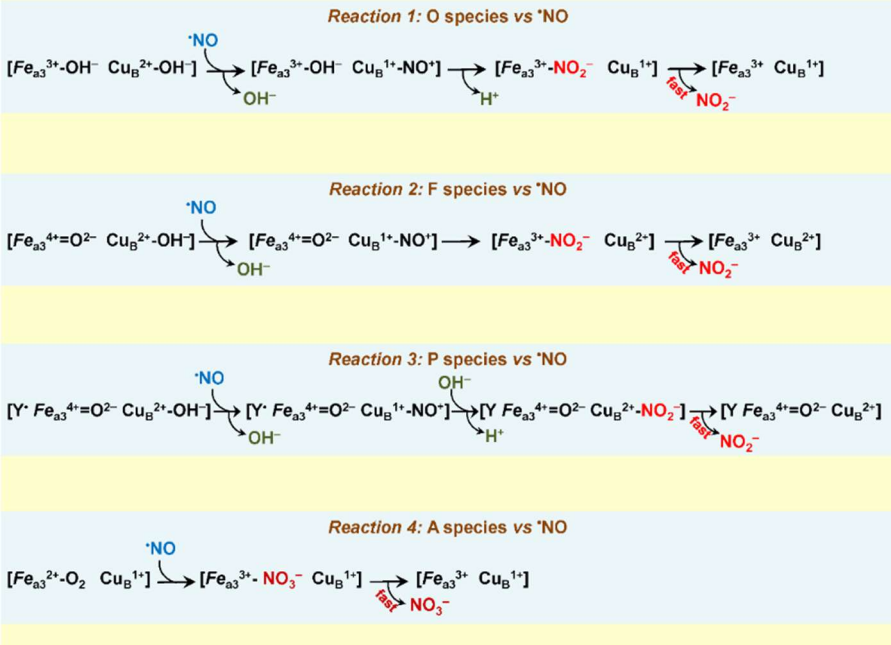

Figure 4. Possible mechanisms of the •NO detoxification catalyzed by the mycobacterial cytochrome *bcc-aa*$_3$ supercomplex under turnover conditions. Y in *Reaction 3*—a conserved tyrosine residue in the BNC.

Since the *bcc-aa*$_3$ is an O_2-binding heme protein, it cannot be ruled out that the enzyme is also capable of acting as a •NO dioxygenase. A possible mechanism of such reaction similar to that reported for the truncated hemoglobin N of *M. tuberculosis* [144] is shown in Figure 4 (reaction 4). According to the proposed pathway, the reaction of the catalytic intermediate A with •NO yields nitrate (NO_3^-) that should leave the BNC rapidly in order to avoid inhibition of the main O_2 reductase activity. All proposed reaction mechanisms (Figure 4, reactions 1–4) await experimental confirmation.

3.1.2. •NO Reductase Activity of Heme–Copper Oxidases

The amperometric studies showed that a few bacterial heme–copper oxidases are able to decompose •NO under reducing anaerobic conditions at •NO concentrations in the solution in the range of 5 to 10 μM. Figure 5 demonstrates such activity of the purified mycobacterial *bcc-aa*$_3$ supercomplex [57]. The pre-reduced enzyme was anaerobically added to an O_2-free solution of •NO in the presence of excess DTT and MD. The addition of the enzyme was shown to increase the rate of the decomposition of •NO. It has to be noted that the slow •NO decay observed before the addition of the *bcc-aa*$_3$ is due to the non-enzymatic reaction of •NO with the reductants. Additionally, the initial fast drop in the •NO concentra-

tion detected immediately after the addition of the enzyme is probably due to •NO binding to the *bcc-aa*$_3$. The •NO-consuming activity of the *bcc-aa*$_3$ under anaerobic conditions at ~8 μM •NO added appeared to be about 3 mol •NO × (mol *bcc-aa*$_3$)$^{-1}$ × min^{-1} [57] (Table 3). As one can see, this is ~100 times lower than that observed under aerobic turnover conditions. A similar activity was also reported previously for such heme–copper oxidases as the *ba*$_3$ and *caa*$_3$ from *Thermus thermophilus* [145], the *bo*$_3$ from *E. coli* [146], the *cbb*$_3$ from *Pseudomonas stutzeri* [147] and *R. sphaeroides* [148]. Notably, the mitochondrial beef heart *aa*$_3$-type oxidase does not catalyze the anaerobic degradation of •NO [149].

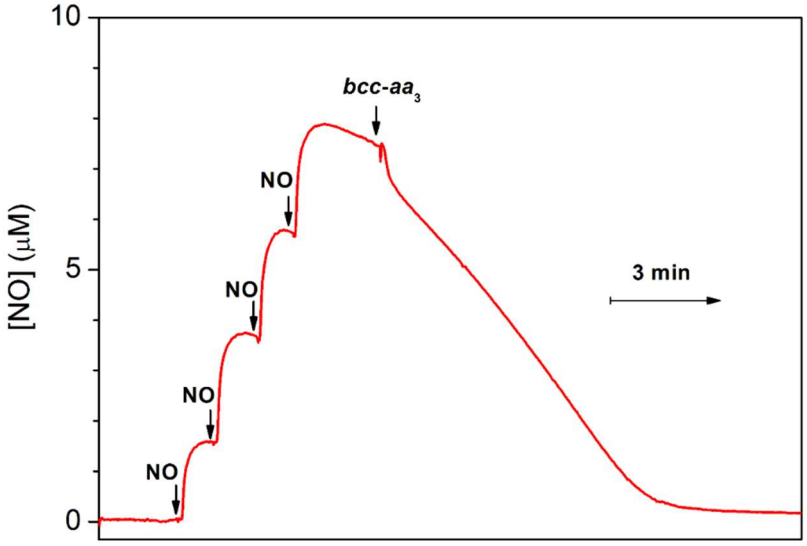

Figure 5. •NO reductase activity of the mycobacterial cytochrome *bcc-aa*$_3$ supercomplex. Four aliquots of 2.1 μM •NO were sequentially added to degassed buffer containing 5 mM DTT, 0.26 mM MD, 5 mM glucose, and 16 units/mL glucose oxidase. Then, the pre-reduced cytochrome *bcc-aa*$_3$ (200 nM) was added. The Figure was modified from Forte et al. [57] under the terms of the Creative Commons Attribution 4.0 International License.

For the *ba*$_3$ oxidase from *T. thermophilus* it was directly shown by gas chromatography that the end product of the catalytic •NO decay under reducing anaerobic conditions is nitrous oxide (N_2O), i.e., the •NO reductase activity takes place [145]. It is reasonable to suggest that this is also the case for the other bacterial oxidases, which were reported to degrade •NO under the same conditions [57,146,148]. The reaction mechanism could resemble that used by native bacterial •NO reductases. Both mechanisms, however, are still under debate [150,151]. In general, two •NO molecules react with the fully reduced BNC of the oxidase yielding one molecule of N_2O as the end product, with the formation of the hyponitrite species as a transient intermediate. For more details, see Figure 23 in [151].

Since the •NO reductase activity measured in some bacterial oxidases is not too high and the conditions requested hardly often occurs in vivo, we do not expect that this contributes significantly to microbial defense mechanisms against •NO-induced stress.

3.2. bd-Type Oxidases Confer Bacterial Resistance to •NO

Evidence is accumulating that in at least some pathogenic bacteria, cytochrome *bd* is involved in their defense against •NO-induced stress. Jones-Carson et al. examined the role of the two major terminal oxidases of *Salmonella* Typhimurium, the heme–copper cytochrome *bo*$_3$ (encoded by the *cyoABCD* operon) and cytochrome *bd* (encoded by the *cydAB* operon), in its antinitrosative defensive system [152]. The authors compared growth rates of the wild-type strain, Δ*cyoABCD*, and Δ*cydAB* mutants in LB broth supplemented with 5 mM DETA NONOate. The latter is the •NO donor that at the added concentration produced a stable flux of 5 μM •NO during the experiment. In contrast to the wild-type and Δ*cyoABCD* strains, the Δ*cydAB* mutant appeared to be hypersusceptible to •NO as

manifested by the extended lag phase following the DETA NONOate addition. Jones-Carson et al. also compared the rates of respiration in the wild-type, Δ*cyoABCD,* and Δ*cydAB* bacterial cultures treated with 50 μM spermine NONOate. The O_2 consumption activity of the Δ*cydAB* mutant was much more sensitive to spermine NONOate as compared to that of the wild-type bacteria. Additionally, unlike the wild-type and Δ*cyoABCD* cells, the O_2 consuming activity of the Δ*cydAB* cells did not improve over time following the addition of spermine NONOate. Cytochrome *bd* was reported to add to the •NO-detoxifying activity of the flavohemoglobin Hmp that converts •NO into NO_3^-. Both Hmp and the *bd* oxidase contribute to similar extents to *S.* Typhimurium pathogenesis. Furthermore, there is a substantial degree of independence between these two proteins in *S.* Typhimurium pathogenesis. It is suggested that low O_2 levels in mice favor •NO detoxification by cytochrome *bd* whereas high O_2 tension favor Hmp as the •NO-detoxifier. Bacteria may experience different O_2 and •NO levels as the inflammatory response evolves over time during the infection. Therefore, *S.* Typhimurium may preferentially use Hmp or the *bd* oxidase according to the availability of O_2 and •NO. Thus, cytochrome *bd*, along with Hmp, is an important component of the antinitrosative defensive system of *S.* Typhimurium [152].

Shepherd et al. examined the relative contribution of cytochrome *bd*-I (CydAB), Hmp, the flavorubredoxin NorVW, the nitrite reductase NrfA, and the iron–sulfur cluster repair protein YtfE to the •NO-tolerance mechanisms in a multidrug-resistant uropathogenic *E. coli* (UPEC), strain EC958 [153]. For this purpose, the authors mutated the *cydAB*, *hmp*, *norVW*, *nrfA* and *ytfE* genes in EC958. Growth rates of wild-type EC958, and *cydAB*, *hmp*, *norVW*, *nrfA* and *ytfE* mutants were measured following the addition of the •NO-releaser NOC-12 under microaerobic conditions. It turned out that mutation of *cydAB* and *hmp* confers the highest sensitivity to •NO. Furthermore, the Δ*cydAB* mutant displayed increased sensitivity to neutrophil killing, reduced survival within primed macrophages, and an attenuated colonization phenotype in the mouse bladder. The fact that deletion of *cydAB* impairs survival in a mouse model suggests that the *bd* oxidase-dependent respiration under nitrosative stress conditions is a key factor for host colonization. Thus, the UPEC cytochrome *bd*-I provides the greatest contribution to •NO tolerance and host colonization at low O_2 tensions and is of major importance for the accumulation of high microbial loads in the course of infection of the urinary tract [153].

Beebout et al. reported that cytochrome *bd* of UPEC (*E. coli* cystitis isolate UTI89) is highly expressed in biofilms and that loss of the *bd*-oxidase-expressing subpopulation impairs barrier function and reduces the abundance of extracellular matrix [154]. The authors hypothesized that cytochrome *bd* is preferentially expressed in the UPEC biofilm because the enzyme provides protection against nitrosative stress. The addition of the •NO donor NOC-12 to planktonic cultures was found to significantly reduce the growth rate of the Δ*cydAB* mutant: the doubling time increased from 37 to 106 min after the treatment. This finding suggests that during aerobic growth the *bd* oxidase serves as an •NO sink that reversibly sequesters •NO. This protects respiration mediated by cytochrome bo_3 which is a proton pump that is more efficient at transducing energy but susceptible to irreversible inhibition by •NO. Beebout et al. proposed that cytochrome *bd*-expressing subpopulations in UPEC are critical for withstanding such harmful metabolic by-products as •NO while in the biofilm state [154].

Consistently, •NO caused more significant growth inhibition in non-pathogenic *E. coli* strains lacking cytochrome *bd* as compared to cytochrome bo_3-deficient ones [155]. In *Shewanella oneidensis*, the *bd* oxidase provides tolerance to nitrite rather than •NO, but this is an exceptional case [156]. A protective role of cytochrome *bd* against •NO stress also agrees with the expression of this enzyme in *E. coli* [154,157,158], *S.* Typhimurium [152], *Staphylococcus aureus* [159], *Bacillus subtilis* [160], and *M. tuberculosis* [161] in response to •NO. Interestingly, in *M. tuberculosis*, the *bd* oxidase was reported to be necessary for optimal respiration at acidic pH as the *bcc-aa*$_3$ supercomplex is markedly inhibited under these conditions [162].

Like most heme–copper oxidases tested (see Section 3.1), the *bd*-type oxidases from non-pathogenic *E. coli* and *A. vinelandii* are rapidly inhibited by •NO [142]. This was demonstrated on the level of both the purified enzymes from these bacteria [142] and the *E. coli* cells lacking cytochrome bo_3 [155,163]. The inhibition is reversible with the IC_{50} value of 100 nM •NO for the purified *bd* oxidases from *E. coli* and *A. vinelandii* at 70 μM O_2 in the assay medium [142] (Table 3). Unlike some heme–copper oxidases (see Section 3.1.2), cytochrome *bd* does not exhibit a measurable •NO reductase activity under anaerobic conditions. The question arises as to if cytochrome *bd* is quickly inhibited by submicromolar concentrations of •NO and unable even scavenge this RNS via •NO reductase-like reaction, how can it serve as one of the key mechanisms for protecting bacteria against nitrosative stress? Phenomenologically, the answer to this question can be obtained by comparing the kinetic profiles of activity recovery from •NO inhibition following the addition of the •NO scavenger oxyhemoglobin (HbO_2) for the *bd* oxidase and the mitochondrial cytochrome *c* oxidase (Figure 6). Upon •NO depletion in solution by HbO_2, the recovery is significantly faster in cytochrome *bd* than in the mitochondrial oxidase under similar experimental conditions [142,164]. However, what molecular mechanisms underlie such a rapid recovery of activity in the case of the *bd* oxidase? Studies of the interaction of •NO with different cytochrome *bd* species made it possible to shed light on the molecular mechanisms [142,143,165,166]. •NO binds at the level of the heme *d* active site. The reaction occurs if heme *d* is in the ferrous, ferryl, or ferric state. The rate of •NO binding to the ferrous uncomplexed heme *d* (R species) has never been measured. One may expect that its value (k_{on}) is comparable with those for the binding of CO and O_2 to the fully reduced enzyme, i.e., in the range of 10^8 to 10^9 $M^{-1}{\cdot}s^{-1}$ [101]. The reaction yields the nitrosyl ferrous heme *d* adduct (Figure 7, reaction 1) [72]. It turned out that the rate of •NO dissociation from heme d^{2+} (k_{off}) in the purified fully reduced cytochrome *bd*-I of *E. coli* is unusually high, 0.133 s^{-1} [143] (Table 3). A similar value (0.163 s^{-1}) was later reported for membrane preparations of *E. coli* mutant strain RKP4544 devoid of cytochrome bo_3 [155]. This k_{off} value is about 30 times higher than that for •NO dissociation from ferrous heme a_3 in the mitochondrial cytochrome *c* oxidase [164]. Furthermore, the •NO off-rate for cytochrome *bd* is faster than that detected for almost all heme proteins. Such a high •NO dissociation rate obviously explains why after •NO-inhibition the activity of cytochrome *bd* is restored much faster than that of the mitochondrial oxidase (Figure 6). The reaction of •NO with the *A. vinelandii* cytochrome *bd* in the ferryl state (F species) is fast (~10^5 $M^{-1}{\cdot}s^{-1}$) and likely produces the oxidized enzyme with nitrite bound at ferric heme *d* (Figure 7, reaction 2) [165]. This is about 10 times faster than the same reaction for the mitochondrial cytochrome *c* oxidase (~10^4 $M^{-1}{\cdot}s^{-1}$) [138,167]. Then, NO_2^- likely escapes from heme d^{3+} to the bulk phase, but the off rate for nitrite has to be determined. Since intermediate F is highly populated in turnover [105], we think that the rapid oxidation of •NO into NO_2^- by cytochrome *bd* also contributes to the mechanisms of bacterial resistance to •NO. The reaction of •NO with ferric heme *d* in the purified fully oxidized cytochrome *bd*-I of *E. coli* (O species) proceeds with k_{on} of ~ 10^2 $M^{-1}{\cdot}s^{-1}$ yielding a nitrosyl adduct, d^{3+}–NO or d^{2+}–NO^+ (Figure 7, reaction 3) [166]. The reaction is rather slow and the O species is not a catalytic intermediate of cytochrome *bd* [168] therefore it barely contributes to mechanisms of •NO-inhibition or •NO tolerance. Thus, we can conclude that the *bd* oxidase confers •NO resistance to bacteria due to (i) extraordinary high •NO off-rate and (ii) the ability to rapidly convert •NO into NO_2^- in turnover.

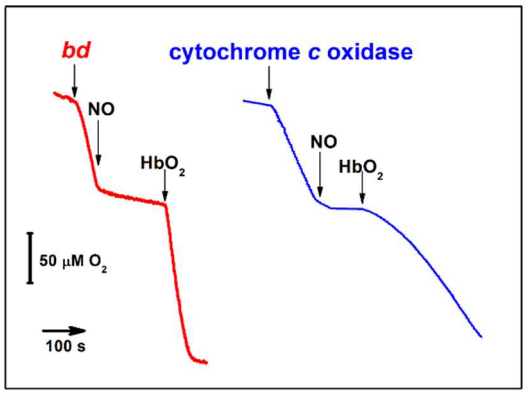

Figure 6. Activity recovery from •NO inhibition of *E. coli* cytochrome *bd*-I and beef heart cytochrome *c* oxidase. Shown are time courses of O_2 consumption by the enzymes. •NO inhibits the enzymatic O_2 consumption. Oxyhemoglobin (HbO_2) scavenges rapidly all free •NO that leads to reversal of •NO inhibition. Modified from [111] with permission.

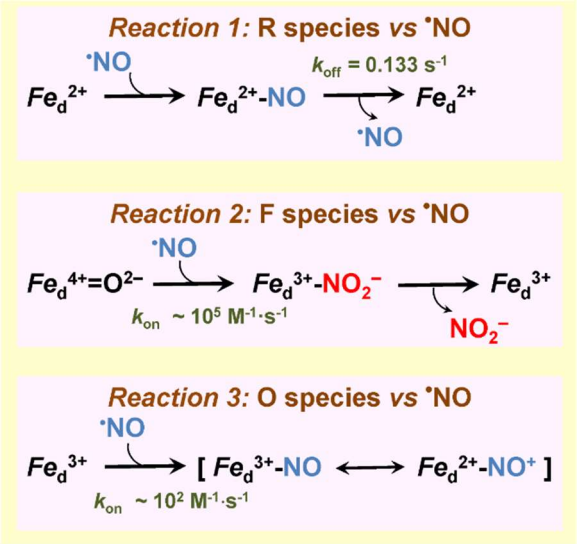

Figure 7. Reactions of •NO with different cytochrome *bd* species.

4. Peroxynitrite and Bacterial Terminal Oxidases

The study of the interaction of peroxynitrite with bacterial terminal oxidases is at the very initial stage. To date, the only bacterial oxidase that has been studied for the reaction with this highly reactive toxic compound is cytochrome *bd*-I from *E. coli* [109,169]. Earlier, the interaction of the eukaryotic heme–copper oxidase, the aa_3-type cytochrome *c* oxidase isolated from bovine heart mitochondria, with $ONOO^-$ was investigated [170]. It was shown that the mitochondrial enzyme when solubilized or in proteoliposomes is irreversibly damaged by $ONOO^-$ (Table 4). At concentrations of less than 20 μM $ONOO^-$ significantly raises the enzyme's K_m for O_2. This effect was tentatively explained by the nitration of some tyrosine residues [137]. At higher concentrations $ONOO^-$ was reported to decrease the V_{max}. The $ONOO^-$-induced lowering of the V_{max} could be due to both the destruction of the Cu_A site in cytochrome *c* oxidase, and the irreversible loss of the 830-nm absorption band characteristic of the oxidized Cu_A was observed [170], and the degradation of hemes *a* and a_3.

Table 4. Overview of $ONOO^-$ interactions with bovine heart aa_3-type cytochrome *c* oxidase and *E. coli* cytochrome *bd*-I.

Enzyme Complex	Inhibition by $ONOO^-$	•NO Production after $ONOO^-$ Addition	Short-Term Generation of O_2 just after $ONOO^-$ Addition	Direct Observation of $ONOO^-$ Degradation in Turnover	Reference
Purified bovine heart aa_3-type cytochrome *c* oxidase	Yes (irreversible damage to enzyme complex)	Yes	No	No	[170]
Purified *E. coli* cytochrome *bd*-I	No (up to 0.1 mM $ONOO^-$)	Yes	Yes	Yes (~600 mol $ONOO^-$ × (mol *bd*-I)$^{-1}$ × min^{-1})	[169]

Borisov et al. studied amperometrically the effect of $ONOO^-$ on the O_2 consumption by the *E. coli* cytochrome *bd*-I at the level of the isolated detergent-solubilized enzyme and the *bd*-I overexpressing bacterial cells [169]. It turned out that in both cases, the O_2 consumption by the *bd*-I oxidase is not inhibited by up to 0.1 mM $ONOO^-$ (Figure 8, Table 4). The effect of higher $ONOO^-$ concentrations was not tested. After the addition of $ONOO^-$ a slight short-term generation of O_2 was observed (Figure 8). This is likely due to the catalase-like activity of cytochrome *bd*-I that scavenges H_2O_2, a contaminant in the commercial $ONOO^-$ or a product of the peroxynitrite degradation [109,113,114]. Furthermore, using the stopped-flow rapid mixing technique it was shown that the *bd*-I oxidase is able to catalyze scavenging of $ONOO^-$. The kinetics of this reaction was measured [169]. In these experiments, the enzyme pre-reduced anaerobically with excess reducing agents, *N*,*N*,*N*′,*N*′-tetramethyl-*p*-phenylenediamine (TMPD), and ascorbate, was mixed with an air-equilibrated solution of $ONOO^-$. The $ONOO^-$ decomposition rate was determined at 310 nm. It was found that $ONOO^-$ disappears with an observed rate constant that is proportional to the cytochrome *bd*-I concentration and increases with the TMPD concentration. Importantly, in control experiments, neither the protein nor the reductants tested independently reveal the decay of $ONOO^-$ to a significant extent. The apparent turnover rate at which the *bd*-I oxidase, in turnover with O_2 and excess TMPD and ascorbate, decomposes $ONOO^-$, was estimated to be ~600 mol $ONOO^-$ × (mol enzyme)$^{-1}$ × min^{-1} [169] (Table 4). Since the rate constant was found to increase with the enzyme activity (the electron flux), in the bacterial cell in which cytochrome *bd*-I utilizes ubiquinol as the substrate, the peroxynitrite-decomposing activity may be even higher. For instance, a turnover number of cytochrome *bd*-I is about seven times higher when the reducing system is ubiquinone-1 plus DTT as compared to that for TMPD plus ascorbate [168]. If the peroxynitrite-neutralizing activity of the *bd*-I oxidase is proportional to the electron flux, its apparent turnover rate in the *E. coli* cell could be as high as ~4200 mol $ONOO^-$ × (mol enzyme)$^{-1}$ × min^{-1}. To summarize, the *E. coli* cytochrome *bd*-I in the catalytic steady state is not only resistant not $ONOO^-$, but also capable of decomposing this highly reactive cytotoxic effector, thus serving as an important detoxifier of $ONOO^-$ in vivo.

A possible mechanism of the peroxynitrite decomposition catalyzed by the *bd*-I enzyme has never been proposed. We assume that the most likely site for the reaction is the high-spin heme *d*. We may suggest at least four possible reaction mechanisms. The fact that the addition of $ONOO^-$ to the isolated *bd*-I protein in turnover with O_2 and reductants resulted in the production of •NO [169] (Table 4) points out that •NO could be the main product. If this is the case, a one-electron reduction of $ONOO^-$ to •NO and H_2O_2 by the ferrous heme *d* may occur (Figure 9, reaction 1). If so, at least part of the H_2O_2 transiently generated following the addition of $ONOO^-$ to the enzyme is also the main reaction product. There are two observations that are not consistent with the mechanism proposed. According to the reaction scheme (Figure 9, reaction 1), the decay of one molecule of $ONOO^-$ added should generate one molecule of •NO. In the experiments, however, the amount of •NO produced was approximately 12 times less than the amount of $ONOO^-$ added. In addition, no •NO production was detected with the $ONOO^-$–treated cells while the short-term generation of H_2O_2 is in place (Figure 8). The latter two findings indicate that the •NO produced in the case of the isolated enzyme might be a secondary product, possibly non-

enzymatic because the formation of •NO was also observed in the absence of the protein, albeit to a lesser extent [169].

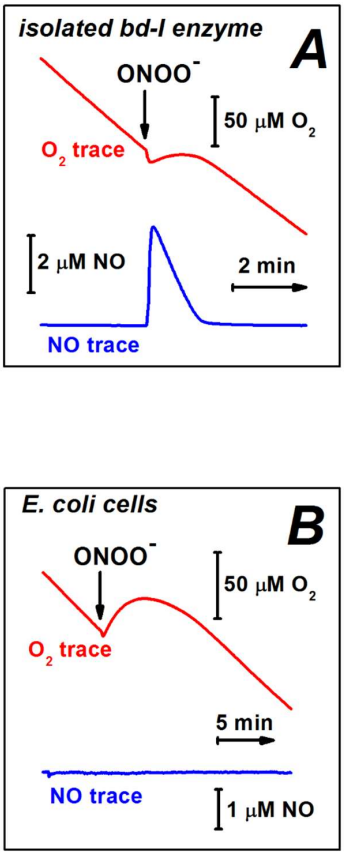

Figure 8. The effect of peroxynitrite on the O_2 consumption by cytochrome *bd*-I from *E. coli*. (**A**) 50 μM $ONOO^-$ was added to the isolated enzyme in the presence of 10 mM ascorbate and 0.5 mM TMPD. (**B**) 80 μM $ONOO^-$ was added to the cell suspension of the *E. coli* strain GO105/pTK1 overexpressing cytochrome *bd*-I. The •NO concentration was measured in parallel. Modified from [169] with permission.

Reaction 1

$$Fe_d^{2+} + ONOO^- + 2H^+ \longrightarrow Fe_d^{3+} + {}^{\bullet}NO + H_2O_2$$

Reaction 2

$$Fe_d^{3+} + ONOO^- \longrightarrow Fe_d^{4+}{=}O^{2-} + {}^{\bullet}NO_2$$

Reaction 3

$$Fe_d^{3+} + ONOO^- \longrightarrow [Fe_d^{4+}{=}O^{2-} \quad {}^{\bullet}NO_2] \longrightarrow Fe_d^{3+} + NO_3^-$$

Reaction 4

$$Fe_d^{3+}\,Por_d + ONOO^- \longrightarrow Fe_d^{4+}{=}O^{2-}\,Por_d^{\bullet+} + NO_2^-$$

Figure 9. Possible mechanisms of the peroxynitrite decomposition catalyzed by cytochrome *bd*-I from *E. coli*.

It was reported that $ONOO^-$ generates Compound II ($Fe^{4+} = O^{2-}$) in myeloperoxidase, lactoperoxidase, and catalase, and Compound I ($Fe^{4+} = O^{2-}$ $Por^{\bullet+}$, where $Por^{\bullet+}$ is a porphyrin radical) in horseradish peroxidase [171,172]. Since these are ferriheme (Fe^{3+}) enzymes, in these reactions $ONOO^-$ serves as a one-electron and two-electron oxidant, respectively. We, therefore, suggest that in cytochrome *bd*-I $ONOO^-$ also could react with the ferric heme *d*, (e.g., to the O^1 catalytic intermediate, see Figure 2). In the case of one-electron oxidation heme d^{3+} is converted to Compound F (analog of Compound II, see Figure 2) with the concomitant release of $^{\bullet}NO_2$ from $ONOO^-$ (Figure 9, reaction 2).

It is also possible that the ferric heme *d* catalyzes the isomerization of peroxynitrite to nitrate (NO_3^-). If so, Compound F and $^{\bullet}NO_2$ are transient reaction intermediates, not the final products (Figure 9, reaction 3). The fact that certain iron (III) porphyrins are capable of catalyzing the isomerization of $ONOO^-$ to NO_3^- [173] is in agreement with this hypothesis.

In the case of two-electron oxidation heme d^{3+} is converted to Compound F* (analog of Compound I, see Figure 2) with the co-production of NO_2^- from $ONOO^-$ (Figure 9, reaction 4). It is worth noting that microbial and mammalian peroxiredoxins catalyze detoxification of peroxynitrite via its two-electron reduction to nitrite [174,175].

5. Concluding Remarks

Usually, terminal oxygen reductases of bacterial respiratory chains are strongly inhibited by nitric oxide and peroxynitrite. However, some of the respiratory enzymes, such as the mycobacterial *bcc-aa*$_3$ supercomplex and *bd*-type oxidases, confer resistance to RNS, thereby contributing to microbial pathogenicity. An understanding of the molecular mechanisms of bacterial pathogenicity is essential for the development of new strategies to combat infectious diseases. In this regard, it would be interesting to figure out the reaction mechanisms underlying *bcc-aa*$_3$ supercomplex-mediated $^{\bullet}NO$ detoxification and importantly, whether this unique property of the mycobacterial enzyme is shared by other *aa*$_3$-type oxidases, eventually complexed with the *bc*$_1$. The interest in *bd*-type oxidases is increasing due to their peculiar enzymatic abilities, stress tolerance, and importance to pathogens—features that merit more in-depth functional and structural studies. Determination of cytochrome *bd* structure from different microorganisms would help in the characterization and rational design of selective inhibitors of these oxidases. Based on already published 3D structures of *bd*-type oxidases, one of the main challenges in the structure-driven design of quinone substrate-like inhibitors is expected to be the high flexibility of the N-terminal part of the quinol binding site called the Q-loop. Another promising direction for future research is the study of the effect of RNS on the anaerobic terminal reductases and other bioenergetic enzymes in anaerobic pathogenic bacteria. All in all, the development of next-generation antibiotics selectively targeting the RNS-insensitive respiratory complexes in pathogens may reduce their impact on human health and social development.

Author Contributions: V.B.B. and E.F. performed the literature review and wrote the paper. All authors have read and agreed to the published version of the manuscript.

Funding: This work was funded by the Russian Science Foundation (project № 22-24-00045, https://rscf.ru/en/project/22-24-00045/ (accessed on 4 June 2022).

Institutional Review Board Statement: Not applicable.

Informed Consent Statement: Not applicable.

Data Availability Statement: Not applicable.

Conflicts of Interest: The authors declare no conflict of interest. The funders had no role in the design of the study; in the collection, analyses, or interpretation of data; in the writing of the manuscript, or in the decision to publish the results.

References

1. Martinez, M.C.; Andriantsitohaina, R. Reactive nitrogen species: Molecular mechanisms and potential significance in health and disease. *Antioxid. Redox Signal.* **2009**, *11*, 669–702. [CrossRef] [PubMed]
2. Wareham, L.K.; Southam, H.M.; Poole, R.K. Do nitric oxide, carbon monoxide and hydrogen sulfide really qualify as 'gasotransmitters' in bacteria? *Biochem. Soc. Trans.* **2018**, *46*, 1107–1118. [CrossRef]
3. Bryan, N.S.; Lefer, D.J. Update on gaseous signaling molecules nitric oxide and hydrogen sulfide: Strategies to capture their functional activity for human therapeutics. *Mol. Pharmacol.* **2019**, *96*, 109–114. [CrossRef] [PubMed]
4. Mendes, S.S.; Miranda, V.; Saraiva, L.M. Hydrogen sulfide and carbon monoxide tolerance in bacteria. *Antioxidants* **2021**, *10*, 729. [CrossRef] [PubMed]
5. Borisov, V.B.; Forte, E. Impact of hydrogen sulfide on mitochondrial and bacterial bioenergetics. *Int. J. Mol. Sci.* **2021**, *22*, 12688. [CrossRef] [PubMed]
6. Radi, R. Oxygen radicals, nitric oxide, and peroxynitrite: Redox pathways in molecular medicine. *Proc. Natl. Acad. Sci. USA* **2018**, *115*, 5839–5848. [CrossRef] [PubMed]
7. Perez de la Lastra, J.M.; Juan, C.A.; Plou, F.J.; Perez-Lebena, E. The nitration of proteins, lipids and DNA by peroxynitrite derivatives-chemistry involved and biological relevance. *Stresses* **2022**, *2*, 3. [CrossRef]
8. Fang, F.C.; Vazquez-Torres, A. Reactive nitrogen species in host-bacterial interactions. *Curr. Opin. Immunol.* **2019**, *60*, 96–102. [CrossRef]
9. Carvalho, S.M.; Beas, J.Z.; Videira, M.A.M.; Saraiva, L.M. Defenses of multidrug resistant pathogens against reactive nitrogen species produced in infected hosts. *Adv. Microb. Physiol.* **2022**, *80*, 85–155. [CrossRef]
10. Gusarov, I.; Nudler, E. Protein S-nitrosylation: Enzymatically controlled, but intrinsically unstable, post-translational modification. *Mol. Cell* **2018**, *69*, 351–353. [CrossRef]
11. Srinivasan, V.B.; Mondal, A.; Venkataramaiah, M.; Chauhan, N.K.; Rajamohan, G. Role of *oxyRKP*, a novel LysR-family transcriptional regulator, in antimicrobial resistance and virulence in *Klebsiella pneumoniae*. *Microbiology (Reading)* **2013**, *159*, 1301–1314. [CrossRef] [PubMed]
12. Anes, J.; Dever, K.; Eshwar, A.; Nguyen, S.; Cao, Y.; Sivasankaran, S.K.; Sakalauskaite, S.; Lehner, A.; Devineau, S.; Daugelavicius, R.; et al. Analysis of the oxidative stress regulon identifies *soxS* as a genetic target for resistance reversal in multidrug-resistant *Klebsiella pneumoniae*. *mBio* **2021**, *12*, e0086721. [CrossRef] [PubMed]
13. Way, S.S.; Goldberg, M.B. Clearance of *Shigella flexneri* infection occurs through a nitric oxide-independent mechanism. *Infect. Immun.* **1998**, *66*, 3012–3016. [CrossRef] [PubMed]
14. Rodionov, D.A.; Dubchak, I.L.; Arkin, A.P.; Alm, E.J.; Gelfand, M.S. Dissimilatory metabolism of nitrogen oxides in bacteria: Comparative reconstruction of transcriptional networks. *PLoS Comput. Biol.* **2005**, *1*, e55. [CrossRef] [PubMed]
15. Kint, N.; Alves Feliciano, C.; Martins, M.C.; Morvan, C.; Fernandes, S.F.; Folgosa, F.; Dupuy, B.; Texeira, M.; Martin-Verstraete, I. How the anaerobic enteropathogen *Clostridioides difficile* tolerates low O_2 tensions. *mBio* **2020**, *11*, e01559-01520. [CrossRef]
16. Folgosa, F.; Martins, M.C.; Teixeira, M. The multidomain flavodiiron protein from *Clostridium difficile* 630 is an NADH:oxygen oxidoreductase. *Sci. Rep.* **2018**, *8*, 10164. [CrossRef]
17. Kumar, M.; Adhikari, S.; Hurdle, J.G. Action of nitroheterocyclic drugs against *Clostridium difficile*. *Int. J. Antimicrob. Agents* **2014**, *44*, 314–319. [CrossRef]
18. Caruana, N.J.; Stroud, D.A. The road to the structure of the mitochondrial respiratory chain supercomplex. *Biochem. Soc. Trans.* **2020**, *48*, 621–629. [CrossRef]
19. Cogliati, S.; Cabrera-Alarcon, J.L.; Enriquez, J.A. Regulation and functional role of the electron transport chain supercomplexes. *Biochem. Soc. Trans.* **2021**, *49*, 2655–2668. [CrossRef]
20. Sharma, P.; Maklashina, E.; Cecchini, G.; Iverson, T.M. Crystal structure of an assembly intermediate of respiratory Complex II. *Nat. Commun.* **2018**, *9*, 274. [CrossRef]
21. Hederstedt, L. Molecular biology of *Bacillus subtilis* cytochromes *anno* 2020. *Biochemistry* **2021**, *86*, 8–21. [CrossRef] [PubMed]
22. Melo, A.M.; Teixeira, M. Supramolecular organization of bacterial aerobic respiratory chains: From cells and back. *Biochim. Biophys. Acta* **2016**, *1857*, 190–197. [CrossRef] [PubMed]
23. Kaila, V.R.I.; Wikstrom, M. Architecture of bacterial respiratory chains. *Nat. Rev. Microbiol.* **2021**, *19*, 319–330. [CrossRef] [PubMed]
24. Nuber, F.; Merono, L.; Oppermann, S.; Schimpf, J.; Wohlwend, D.; Friedrich, T. A quinol anion as catalytic intermediate coupling proton translocation with electron transfer in *E. coli* respiratory complex I. *Front. Chem.* **2021**, *9*, 672969. [CrossRef]
25. Grba, D.N.; Blaza, J.N.; Bridges, H.R.; Agip, A.A.; Yin, Z.; Murai, M.; Miyoshi, H.; Hirst, J. Cryo-electron microscopy reveals how acetogenins inhibit mitochondrial respiratory complex I. *J. Biol. Chem.* **2022**, *298*, 101602. [CrossRef]
26. Marreiros, B.C.; Sena, F.V.; Sousa, F.M.; Batista, A.P.; Pereira, M.M. Type II NADH:quinone oxidoreductase family: Phylogenetic distribution, structural diversity and evolutionary divergences. *Environ. Microbiol.* **2016**, *18*, 4697–4709. [CrossRef]
27. Blaza, J.N.; Bridges, H.R.; Aragao, D.; Dunn, E.A.; Heikal, A.; Cook, G.M.; Nakatani, Y.; Hirst, J. The mechanism of catalysis by type-II NADH:quinone oxidoreductases. *Sci. Rep.* **2017**, *7*, 40165. [CrossRef]
28. Bertsova, Y.V.; Baykov, A.A.; Bogachev, A.V. A simple strategy to differentiate between H^+- and Na^+-transporting NADH:quinone oxidoreductases. *Arch. Biochem. Biophys.* **2020**, *681*, 108266. [CrossRef]

29. Liang, P.; Fang, X.; Hu, Y.; Yuan, M.; Raba, D.A.; Ding, J.; Bunn, D.C.; Sanjana, K.; Yang, J.; Rosas-Lemus, M.; et al. The aerobic respiratory chain of *Pseudomonas aeruginosa* cultured in artificial urine media: Role of NQR and terminal oxidases. *PLoS ONE* **2020**, *15*, e0231965. [CrossRef]
30. Hreha, T.N.; Foreman, S.; Duran-Pinedo, A.; Morris, A.R.; Diaz-Rodriguez, P.; Jones, J.A.; Ferrara, K.; Bourges, A.; Rodriguez, L.; Koffas, M.A.G.; et al. The three NADH dehydrogenases of *Pseudomonas aeruginosa*: Their roles in energy metabolism and links to virulence. *PLoS ONE* **2021**, *16*, e0244142. [CrossRef]
31. Kozlova, M.I.; Bushmakin, I.M.; Belyaeva, J.D.; Shalaeva, D.N.; Dibrova, D.V.; Cherepanov, D.A.; Mulkidjanian, A.Y. Expansion of the "Sodium World" through evolutionary time and taxonomic space. *Biochemistry* **2020**, *85*, 1518–1542. [CrossRef] [PubMed]
32. Wilson, C.A.; Crofts, A.R. Dissecting the pattern of proton release from partial process involved in ubihydroquinone oxidation in the Q-cycle. *Biochim. Biophys. Acta Bioenerg.* **2018**, *1859*, 531–543. [CrossRef] [PubMed]
33. Francia, F.; Khalfaoui-Hassani, B.; Lanciano, P.; Musiani, F.; Noodleman, L.; Venturoli, G.; Daldal, F. The cytochrome *b* lysine 329 residue is critical for ubihydroquinone oxidation and proton release at the Q_o site of bacterial cytochrome bc_1. *Biochim. Biophys. Acta Bioenerg.* **2019**, *1860*, 167–179. [CrossRef] [PubMed]
34. Borisov, V.B.; Verkhovsky, M.I. Oxygen as Acceptor. *EcoSal Plus* **2015**, *6*. [CrossRef] [PubMed]
35. Wiseman, B.; Nitharwal, R.G.; Fedotovskaya, O.; Schafer, J.; Guo, H.; Kuang, Q.; Benlekbir, S.; Sjostrand, D.; Adelroth, P.; Rubinstein, J.L.; et al. Structure of a functional obligate complex III_2IV_2 respiratory supercomplex from *Mycobacterium smegmatis*. *Nat. Struct. Mol. Biol.* **2018**, *25*, 1128–1136. [CrossRef] [PubMed]
36. Gong, H.; Li, J.; Xu, A.; Tang, Y.; Ji, W.; Gao, R.; Wang, S.; Yu, L.; Tian, C.; Li, J.; et al. An electron transfer path connects subunits of a mycobacterial respiratory supercomplex. *Science* **2018**, *362*, eaat8923. [CrossRef]
37. Kao, W.C.; Ortmann de Percin Northumberland, C.; Cheng, T.C.; Ortiz, J.; Durand, A.; von Loeffelholz, O.; Schilling, O.; Biniossek, M.L.; Klaholz, B.P.; Hunte, C. Structural basis for safe and efficient energy conversion in a respiratory supercomplex. *Nat. Commun.* **2022**, *13*, 545. [CrossRef]
38. Fedotovskaya, O.; Albertsson, I.; Nordlund, G.; Hong, S.; Gennis, R.B.; Brzezinski, P.; Adelroth, P. Identification of a cytochrome bc_1-aa_3 supercomplex in *Rhodobacter sphaeroides*. *Biochim. Biophys. Acta Bioenerg.* **2021**, *1862*, 148433. [CrossRef]
39. Friedrich, T.; Wohlwend, D.; Borisov, V.B. Recent advances in structural studies of cytochrome *bd* and its potential application as a drug target. *Int. J. Mol. Sci.* **2022**, *23*, 3166. [CrossRef]
40. Vilcheze, C.; Weinrick, B.; Leung, L.W.; Jacobs, W.R., Jr. Plasticity of *Mycobacterium tuberculosis* NADH dehydrogenases and their role in virulence. *Proc. Natl. Acad. Sci. USA* **2018**, *115*, 1599–1604. [CrossRef]
41. Siletsky, S.A.; Borisov, V.B. Proton pumping and non-pumping terminal respiratory oxidases: Active sites intermediates of these molecular machines and their derivatives. *Int. J. Mol. Sci.* **2021**, *22*, 10852. [CrossRef] [PubMed]
42. Murali, R.; Gennis, R.B.; Hemp, J. Evolution of the cytochrome *bd* oxygen reductase superfamily and the function of CydAA′ in Archaea. *ISME J.* **2021**, *15*, 3534–3548. [CrossRef] [PubMed]
43. Borisov, V.B.; Siletsky, S.A.; Paiardini, A.; Hoogewijs, D.; Forte, E.; Giuffre, A.; Poole, R.K. Bacterial oxidases of the cytochrome *bd* family: Redox enzymes of unique structure, function and utility as drug targets. *Antioxid. Redox Signal.* **2021**, *34*, 1280–1318. [CrossRef] [PubMed]
44. Siletsky, S.A.; Borisov, V.B.; Mamedov, M.D. Photosystem II and terminal respiratory oxidases: Molecular machines operating in opposite directions. *Front. Biosci. (Landmark Ed.)* **2017**, *22*, 1379–1426. [CrossRef] [PubMed]
45. Malatesta, F.; Antonini, G.; Sarti, P.; Brunori, M. Structure and function of a molecular machine: Cytochrome *c* oxidase. *Biophys. Chem.* **1995**, *54*, 1–33. [CrossRef]
46. Pereira, M.M.; Sousa, F.L.; Verissimo, A.F.; Teixeira, M. Looking for the minimum common denominator in haem-copper oxygen reductases: Towards a unified catalytic mechanism. *Biochim. Biophys. Acta* **2008**, *1777*, 929–934. [CrossRef]
47. Papa, S.; Capitanio, N.; Capitanio, G.; Palese, L.L. Protonmotive cooperativity in cytochrome *c* oxidase. *Biochim. Biophys. Acta* **2004**, *1658*, 95–105. [CrossRef]
48. Borisov, V.B.; Siletsky, S.A. Features of organization and mechanism of catalysis of two families of terminal oxidases: Heme-copper and *bd*-type. *Biochemistry* **2019**, *84*, 1390–1402. [CrossRef]
49. Borisov, V.B.; Siletsky, S.A.; Nastasi, M.R.; Forte, E. ROS defense systems and terminal oxidases in bacteria. *Antioxidants* **2021**, *10*, 839. [CrossRef]
50. Sousa, F.L.; Alves, R.J.; Ribeiro, M.A.; Pereira-Leal, J.B.; Teixeira, M.; Pereira, M.M. The superfamily of heme-copper oxygen reductases: Types and evolutionary considerations. *Biochim. Biophys. Acta* **2012**, *1817*, 629–637. [CrossRef]
51. Wikstrom, M.; Krab, K.; Sharma, V. Oxygen activation and energy conservation by cytochrome *c* oxidase. *Chem. Rev.* **2018**, *118*, 2469–2490. [CrossRef] [PubMed]
52. Capitanio, N.; Palese, L.L.; Capitanio, G.; Martino, P.L.; Richter, O.M.; Ludwig, B.; Papa, S. Allosteric interactions and proton conducting pathways in proton pumping aa_3 oxidases: Heme *a* as a key coupling element. *Biochim. Biophys. Acta* **2012**, *1817*, 558–566. [CrossRef] [PubMed]
53. Maneg, O.; Malatesta, F.; Ludwig, B.; Drosou, V. Interaction of cytochrome *c* with cytochrome oxidase: Two different docking scenarios. *Biochim. Biophys. Acta* **2004**, *1655*, 274–281. [CrossRef] [PubMed]
54. von Ballmoos, C.; Adelroth, P.; Gennis, R.B.; Brzezinski, P. Proton transfer in ba_3 cytochrome *c* oxidase from *Thermus thermophilus*. *Biochim. Biophys. Acta* **2012**, *1817*, 650–657. [CrossRef] [PubMed]

55. Rich, P.R. Mitochondrial cytochrome *c* oxidase: Catalysis, coupling and controversies. *Biochem. Soc. Trans.* **2017**, *45*, 813–829. [CrossRef]
56. Yoshikawa, S.; Shimada, A. Reaction mechanism of cytochrome *c* oxidase. *Chem. Rev.* **2015**, *115*, 1936–1989. [CrossRef]
57. Forte, E.; Giuffre, A.; Huang, L.S.; Berry, E.A.; Borisov, V.B. Nitric oxide does not inhibit but is metabolized by the cytochrome *bcc-aa*$_3$ supercomplex. *Int. J. Mol. Sci.* **2020**, *21*, 8521. [CrossRef]
58. Borisov, V.B. Defects in mitochondrial respiratory complexes III and IV, and human pathologies. *Mol. Aspects Med.* **2002**, *23*, 385–412. [CrossRef]
59. Borisov, V.B. Mutations in respiratory chain complexes and human diseases. *Ital. J. Biochem.* **2004**, *53*, 34–40.
60. Pereira, M.M.; Santana, M.; Teixeira, M. A novel scenario for the evolution of haem-copper oxygen reductases. *Biochim. Biophys. Acta* **2001**, *1505*, 185–208. [CrossRef]
61. Pereira, M.M.; Gomes, C.M.; Teixeira, M. Plasticity of proton pathways in haem-copper oxygen reductases. *FEBS Lett.* **2002**, *522*, 14–18. [CrossRef]
62. Pereira, M.M.; Teixeira, M. Proton pathways, ligand binding and dynamics of the catalytic site in haem-copper oxygen reductases: A comparison between the three families. *Biochim. Biophys. Acta* **2004**, *1655*, 340–346. [CrossRef] [PubMed]
63. Safarian, S.; Rajendran, C.; Muller, H.; Preu, J.; Langer, J.D.; Ovchinnikov, S.; Hirose, T.; Kusumoto, T.; Sakamoto, J.; Michel, H. Structure of a bd oxidase indicates similar mechanisms for membrane-integrated oxygen reductases. *Science* **2016**, *352*, 583–586. [CrossRef]
64. Thesseling, A.; Rasmussen, T.; Burschel, S.; Wohlwend, D.; Kagi, J.; Muller, R.; Bottcher, B.; Friedrich, T. Homologous *bd* oxidases share the same architecture but differ in mechanism. *Nat. Commun.* **2019**, *10*, 5138. [CrossRef] [PubMed]
65. Safarian, S.; Hahn, A.; Mills, D.J.; Radloff, M.; Eisinger, M.L.; Nikolaev, A.; Meier-Credo, J.; Melin, F.; Miyoshi, H.; Gennis, R.B.; et al. Active site rearrangement and structural divergence in prokaryotic respiratory oxidases. *Science* **2019**, *366*, 100–104. [CrossRef]
66. Wang, W.; Gao, Y.; Tang, Y.; Zhou, X.; Lai, Y.; Zhou, S.; Zhang, Y.; Yang, X.; Liu, F.; Guddat, L.W.; et al. Cryo-EM structure of mycobacterial cytochrome *bd* reveals two oxygen access channels. *Nat. Commun.* **2021**, *12*, 4621. [CrossRef]
67. Safarian, S.; Opel-Reading, H.K.; Wu, D.; Mehdipour, A.R.; Hards, K.; Harold, L.K.; Radloff, M.; Stewart, I.; Welsch, S.; Hummer, G.; et al. The cryo-EM structure of the *bd* oxidase from *M. tuberculosis* reveals a unique structural framework and enables rational drug design to combat TB. *Nat. Commun.* **2021**, *12*, 5236. [CrossRef]
68. Grauel, A.; Kagi, J.; Rasmussen, T.; Makarchuk, I.; Oppermann, S.; Moumbock, A.F.A.; Wohlwend, D.; Muller, R.; Melin, F.; Gunther, S.; et al. Structure of *Escherichia coli* cytochrome *bd*-II type oxidase with bound aurachin D. *Nat. Commun.* **2021**, *12*, 6498. [CrossRef]
69. Grund, T.N.; Radloff, M.; Wu, D.; Goojani, H.G.; Witte, L.F.; Josting, W.; Buschmann, S.; Muller, H.; Elamri, I.; Welsch, S.; et al. Mechanistic and structural diversity between cytochrome *bd* isoforms of *Escherichia coli*. *Proc. Natl. Acad. Sci. USA* **2021**, *118*, e2114013118. [CrossRef]
70. Hill, J.J.; Alben, J.O.; Gennis, R.B. Spectroscopic evidence for a heme-heme binuclear center in the cytochrome *bd* ubiquinol oxidase from *Escherichia coli*. *Proc. Natl. Acad. Sci. USA* **1993**, *90*, 5863–5867. [CrossRef]
71. Tsubaki, M.; Hori, H.; Mogi, T.; Anraku, Y. Cyanide-binding site of *bd*-type ubiquinol oxidase from *Escherichia coli*. *J. Biol. Chem.* **1995**, *270*, 28565–28569. [CrossRef] [PubMed]
72. Borisov, V.; Arutyunyan, A.M.; Osborne, J.P.; Gennis, R.B.; Konstantinov, A.A. Magnetic circular dichroism used to examine the interaction of *Escherichia coli* cytochrome *bd* with ligands. *Biochemistry* **1999**, *38*, 740–750. [CrossRef] [PubMed]
73. Vos, M.H.; Borisov, V.B.; Liebl, U.; Martin, J.L.; Konstantinov, A.A. Femtosecond resolution of ligand-heme interactions in the high-affinity quinol oxidase *bd*: A di-heme active site? *Proc. Natl. Acad. Sci. USA* **2000**, *97*, 1554–1559. [CrossRef] [PubMed]
74. Borisov, V.B.; Sedelnikova, S.E.; Poole, R.K.; Konstantinov, A.A. Interaction of cytochrome *bd* with carbon monoxide at low and room temperatures: Evidence that only a small fraction of heme b_{595} reacts with CO. *J. Biol. Chem.* **2001**, *276*, 22095–22099. [CrossRef] [PubMed]
75. Borisov, V.B.; Liebl, U.; Rappaport, F.; Martin, J.L.; Zhang, J.; Gennis, R.B.; Konstantinov, A.A.; Vos, M.H. Interactions between heme *d* and heme b_{595} in quinol oxidase *bd* from *Escherichia coli*: A photoselection study using femtosecond spectroscopy. *Biochemistry* **2002**, *41*, 1654–1662. [CrossRef]
76. Arutyunyan, A.M.; Borisov, V.B.; Novoderezhkin, V.I.; Ghaim, J.; Zhang, J.; Gennis, R.B.; Konstantinov, A.A. Strong excitonic interactions in the oxygen-reducing site of *bd*-type oxidase: The Fe-to-Fe distance between hemes *d* and b_{595} is 10 A. *Biochemistry* **2008**, *47*, 1752–1759. [CrossRef]
77. Borisov, V.B. Interaction of *bd*-type quinol oxidase from *Escherichia coli* and carbon monoxide: Heme *d* binds CO with high affinity. *Biochemistry* **2008**, *73*, 14–22. [CrossRef]
78. Bloch, D.A.; Borisov, V.B.; Mogi, T.; Verkhovsky, M.I. Heme/heme redox interaction and resolution of individual optical absorption spectra of the hemes in cytochrome *bd* from *Escherichia coli*. *Biochim. Biophys. Acta* **2009**, *1787*, 1246–1253. [CrossRef]
79. Rappaport, F.; Zhang, J.; Vos, M.H.; Gennis, R.B.; Borisov, V.B. Heme-heme and heme-ligand interactions in the di-heme oxygen-reducing site of cytochrome *bd* from *Escherichia coli* revealed by nanosecond absorption spectroscopy. *Biochim. Biophys. Acta* **2010**, *1797*, 1657–1664. [CrossRef]
80. Borisov, V.B.; Verkhovsky, M.I. Accommodation of CO in the di-heme active site of cytochrome *bd* terminal oxidase from *Escherichia coli*. *J. Inorg. Biochem.* **2013**, *118*, 65–67. [CrossRef]

81. Siletsky, S.A.; Zaspa, A.A.; Poole, R.K.; Borisov, V.B. Microsecond time-resolved absorption spectroscopy used to study CO compounds of cytochrome *bd* from *Escherichia coli*. *PLoS ONE* **2014**, *9*, e95617. [CrossRef] [PubMed]
82. Siletsky, S.A.; Rappaport, F.; Poole, R.K.; Borisov, V.B. Evidence for fast electron transfer between the high-spin haems in cytochrome *bd*-I from *Escherichia coli*. *PLoS ONE* **2016**, *11*, e0155186. [CrossRef]
83. Siletsky, S.A.; Dyuba, A.V.; Elkina, D.A.; Monakhova, M.V.; Borisov, V.B. Spectral-kinetic analysis of recombination reaction of heme centers of *bd*-type quinol oxidase from *Escherichia coli* with carbon monoxide. *Biochemistry* **2017**, *82*, 1354–1366. [CrossRef]
84. Borisov, V.B. Effect of membrane environment on ligand-binding properties of the terminal oxidase cytochrome *bd*-I from *Escherichia coli*. *Biochemistry* **2020**, *85*, 1603–1612. [CrossRef] [PubMed]
85. Gavrikova, E.V.; Grivennikova, V.G.; Borisov, V.B.; Cecchini, G.; Vinogradov, A.D. Assembly of a chimeric respiratory chain from bovine heart submitochondrial particles and cytochrome *bd* terminal oxidase of *Escherichia coli*. *FEBS Lett.* **2009**, *583*, 1287–1291. [CrossRef] [PubMed]
86. Azarkina, N.; Borisov, V.; Konstantinov, A.A. Spontaneous spectral changes of the reduced cytochrome *bd*. *FEBS Lett.* **1997**, *416*, 171–174. [CrossRef]
87. Puustinen, A.; Finel, M.; Haltia, T.; Gennis, R.B.; Wikstrom, M. Properties of the two terminal oxidases of *Escherichia coli*. *Biochemistry* **1991**, *30*, 3936–3942. [CrossRef]
88. Jasaitis, A.; Borisov, V.B.; Belevich, N.P.; Morgan, J.E.; Konstantinov, A.A.; Verkhovsky, M.I. Electrogenic reactions of cytochrome *bd*. *Biochemistry* **2000**, *39*, 13800–13809. [CrossRef]
89. Belevich, I.; Borisov, V.B.; Zhang, J.; Yang, K.; Konstantinov, A.A.; Gennis, R.B.; Verkhovsky, M.I. Time-resolved electrometric and optical studies on cytochrome *bd* suggest a mechanism of electron-proton coupling in the di-heme active site. *Proc. Natl. Acad. Sci. USA* **2005**, *102*, 3657–3662. [CrossRef]
90. Belevich, I.; Borisov, V.B.; Verkhovsky, M.I. Discovery of the true peroxy intermediate in the catalytic cycle of terminal oxidases by real-time measurement. *J. Biol. Chem.* **2007**, *282*, 28514–28519. [CrossRef]
91. Borisov, V.B.; Belevich, I.; Bloch, D.A.; Mogi, T.; Verkhovsky, M.I. Glutamate 107 in subunit I of cytochrome *bd* from *Escherichia coli* is part of a transmembrane intraprotein pathway conducting protons from the cytoplasm to the heme b_{595}/heme *d* active site. *Biochemistry* **2008**, *47*, 7907–7914. [CrossRef] [PubMed]
92. Borisov, V.B. Cytochrome *bd*: Structure and properties. *Biochemistry* **1996**, *61*, 565–574.
93. Junemann, S. Cytochrome *bd* terminal oxidase. *Biochim. Biophys. Acta* **1997**, *1321*, 107–127. [CrossRef] [PubMed]
94. Forte, E.; Borisov, V.B.; Vicente, J.B.; Giuffre, A. Cytochrome *bd* and gaseous ligands in bacterial physiology. *Adv. Microb. Physiol.* **2017**, *71*, 171–234. [CrossRef] [PubMed]
95. Borisov, V.B.; Smirnova, I.A.; Krasnosel'skaya, I.A.; Konstantinov, A.A. Oxygenated cytochrome *bd* from *Escherichia coli* can be converted into the oxidized form by lipophilic electron acceptors. *Biochemistry* **1994**, *59*, 437–443.
96. D'mello, R.; Hill, S.; Poole, R.K. The cytochrome *bd* quinol oxidase in *Escherichia coli* has an extremely high oxygen affinity and two-oxygen-binding haems: Implicaitons for regulation of activity in vivo by oxygen inihibition. *Microbiology* **1996**, *142*, 755–763. [CrossRef]
97. Belevich, I.; Borisov, V.B.; Konstantinov, A.A.; Verkhovsky, M.I. Oxygenated complex of cytochrome *bd* from *Escherichia coli*: Stability and photolability. *FEBS Lett.* **2005**, *579*, 4567–4570. [CrossRef]
98. Belevich, I.; Borisov, V.B.; Bloch, D.A.; Konstantinov, A.A.; Verkhovsky, M.I. Cytochrome *bd* from *Azotobacter vinelandii*: Evidence for high-affinity oxygen binding. *Biochemistry* **2007**, *46*, 11177–11184. [CrossRef]
99. Forte, E.; Borisov, V.B.; Siletsky, S.A.; Petrosino, M.; Giuffre, A. In the respiratory chain of *Escherichia coli* cytochromes *bd*-I and *bd*-II are more sensitive to carbon monoxide inhibition than cytochrome bo_3. *Biochim. Biophys. Acta Bioenerg.* **2019**, *1860*, 148088. [CrossRef]
100. Azarkina, N.; Siletsky, S.; Borisov, V.; von Wachenfeldt, C.; Hederstedt, L.; Konstantinov, A.A. A cytochrome *bb'*-type quinol oxidase in *Bacillus subtilis* strain 168. *J. Biol. Chem.* **1999**, *274*, 32810–32817. [CrossRef]
101. Borisov, V.B.; Gennis, R.B.; Hemp, J.; Verkhovsky, M.I. The cytochrome *bd* respiratory oxygen reductases. *Biochim. Biophys. Acta* **2011**, *1807*, 1398–1413. [CrossRef] [PubMed]
102. Arutyunyan, A.M.; Sakamoto, J.; Inadome, M.; Kabashima, Y.; Borisov, V.B. Optical and magneto-optical activity of cytochrome *bd* from *Geobacillus thermodenitrificans*. *Biochim. Biophys. Acta* **2012**, *1817*, 2087–2094. [CrossRef] [PubMed]
103. Borisov, V.B.; Gennis, R.B.; Konstantinov, A.A. Interaction of cytochrome *bd* from *Escherichia coli* with hydrogen peroxide. *Biochemistry* **1995**, *60*, 231–239.
104. Borisov, V.; Gennis, R.; Konstantinov, A.A. Peroxide complex of cytochrome *bd*: Kinetics of generation and stability. *Biochem. Mol. Biol. Int.* **1995**, *37*, 975–982.
105. Borisov, V.B.; Forte, E.; Sarti, P.; Giuffre, A. Catalytic intermediates of cytochrome *bd* terminal oxidase at steady-state: Ferryl and oxy-ferrous species dominate. *Biochim. Biophys. Acta* **2011**, *1807*, 503–509. [CrossRef]
106. Paulus, A.; Rossius, S.G.; Dijk, M.; de Vries, S. Oxoferryl-porphyrin radical catalytic intermediate in cytochrome *bd* oxidases protects cells from formation of reactive oxygen species. *J. Biol. Chem.* **2012**, *287*, 8830–8838. [CrossRef]
107. Borisov, V.B.; Murali, R.; Verkhovskaya, M.L.; Bloch, D.A.; Han, H.; Gennis, R.B.; Verkhovsky, M.I. Aerobic respiratory chain of *Escherichia coli* is not allowed to work in fully uncoupled mode. *Proc. Natl. Acad. Sci. USA* **2011**, *108*, 17320–17324. [CrossRef]
108. Forte, E.; Borisov, V.B.; Konstantinov, A.A.; Brunori, M.; Giuffre, A.; Sarti, P. Cytochrome *bd*, a key oxidase in bacterial survival and tolerance to nitrosative stress. *Ital. J. Biochem.* **2007**, *56*, 265–269.

109. Borisov, V.B.; Forte, E.; Siletsky, S.A.; Arese, M.; Davletshin, A.I.; Sarti, P.; Giuffre, A. Cytochrome *bd* protects bacteria against oxidative and nitrosative stress: A potential target for next-generation antimicrobial agents. *Biochemistry* **2015**, *80*, 565–575. [CrossRef]
110. Giuffre, A.; Borisov, V.B.; Mastronicola, D.; Sarti, P.; Forte, E. Cytochrome *bd* oxidase and nitric oxide: From reaction mechanisms to bacterial physiology. *FEBS Lett.* **2012**, *586*, 622–629. [CrossRef]
111. Giuffre, A.; Borisov, V.B.; Arese, M.; Sarti, P.; Forte, E. Cytochrome *bd* oxidase and bacterial tolerance to oxidative and nitrosative stress. *Biochim. Biophys. Acta* **2014**, *1837*, 1178–1187. [CrossRef] [PubMed]
112. Borisov, V.B.; Davletshin, A.I.; Konstantinov, A.A. Peroxidase activity of cytochrome *bd* from *Escherichia coli*. *Biochemistry* **2010**, *75*, 428–436. [CrossRef] [PubMed]
113. Borisov, V.B.; Forte, E.; Davletshin, A.; Mastronicola, D.; Sarti, P.; Giuffre, A. Cytochrome *bd* oxidase from *Escherichia coli* displays high catalase activity: An additional defense against oxidative stress. *FEBS Lett.* **2013**, *587*, 2214–2218. [CrossRef] [PubMed]
114. Forte, E.; Borisov, V.B.; Davletshin, A.; Mastronicola, D.; Sarti, P.; Giuffre, A. Cytochrome *bd* oxidase and hydrogen peroxide resistance in *Mycobacterium tuberculosis*. *mBio* **2013**, *4*, e01006-01013. [CrossRef]
115. Al-Attar, S.; Yu, Y.; Pinkse, M.; Hoeser, J.; Friedrich, T.; Bald, D.; de Vries, S. Cytochrome *bd* displays significant quinol peroxidase activity. *Sci. Rep.* **2016**, *6*, 27631. [CrossRef] [PubMed]
116. Forte, E.; Nastasi, M.R.; Borisov, V.B. Preparations of terminal oxidase cytochrome *bd*-II isolated from *Escherichia coli* reveal significant hydrogen peroxide scavenging activity. *Biochemistry*, 2022; *in press*.
117. Forte, E.; Borisov, V.B.; Falabella, M.; Colaco, H.G.; Tinajero-Trejo, M.; Poole, R.K.; Vicente, J.B.; Sarti, P.; Giuffre, A. The terminal oxidase cytochrome *bd* promotes sulfide-resistant bacterial respiration and growth. *Sci. Rep.* **2016**, *6*, 23788. [CrossRef]
118. Korshunov, S.; Imlay, K.R.; Imlay, J.A. The cytochrome *bd* oxidase of *Escherichia coli* prevents respiratory inhibition by endogenous and exogenous hydrogen sulfide. *Mol. Microbiol.* **2016**, *101*, 62–77. [CrossRef]
119. Forte, E.; Giuffre, A. How bacteria breathe in hydrogen sulphide-rich environments. *Biochemist* **2016**, *38*, 8–11. [CrossRef]
120. Borisov, V.B.; Forte, E. Terminal oxidase cytochrome *bd* protects bacteria against hydrogen sulfide toxicity. *Biochemistry* **2021**, *86*, 22–32. [CrossRef]
121. Forte, E.; Siletsky, S.A.; Borisov, V.B. In *Escherichia coli* ammonia inhibits cytochrome bo_3 but activates cytochrome *bd*-I. *Antioxidants* **2021**, *10*, 13. [CrossRef]
122. Xia, X.; Wu, S.; Li, L.; Xu, B.; Wang, G. The cytochrome *bd* complex is essential for chromate and sulfide resistance and is regulated by a GbsR-type regulator, CydE, in *Alishewanella* sp. WH16-1. *Front. Microbiol.* **2018**, *9*, 1849. [CrossRef] [PubMed]
123. Sakamoto, J.; Koga, E.; Mizuta, T.; Sato, C.; Noguchi, S.; Sone, N. Gene structure and quinol oxidase activity of a cytochrome *bd*-type oxidase from *Bacillus stearothermophilus*. *Biochim. Biophys. Acta* **1999**, *1411*, 147–158. [CrossRef]
124. Kalia, N.P.; Hasenoehrl, E.J.; Ab Rahman, N.B.; Koh, V.H.; Ang, M.L.T.; Sajorda, D.R.; Hards, K.; Gruber, G.; Alonso, S.; Cook, G.M.; et al. Exploiting the synthetic lethality between terminal respiratory oxidases to kill *Mycobacterium tuberculosis* and clear host infection. *Proc. Natl. Acad. Sci. USA* **2017**, *114*, 7426–7431. [CrossRef] [PubMed]
125. Lee, B.S.; Hards, K.; Engelhart, C.A.; Hasenoehrl, E.J.; Kalia, N.P.; Mackenzie, J.S.; Sviriaeva, E.; Chong, S.M.S.; Manimekalai, M.S.S.; Koh, V.H.; et al. Dual inhibition of the terminal oxidases eradicates antibiotic-tolerant *Mycobacterium tuberculosis*. *EMBO Mol. Med.* **2021**, *13*, e13207. [CrossRef] [PubMed]
126. Meunier, B.; Madgwick, S.A.; Reil, E.; Oettmeier, W.; Rich, P.R. New inhibitors of the quinol oxidation sites of bacterial cytochromes *bo* and *bd*. *Biochemistry* **1995**, *34*, 1076–1083. [CrossRef]
127. Radloff, M.; Elamri, I.; Grund, T.N.; Witte, L.F.; Hohmann, K.F.; Nakagaki, S.; Goojani, H.G.; Nasiri, H.; Hideto, M.; Bald, D.; et al. Short-chain aurachin D derivatives are selective inhibitors of *E. coli* cytochrome *bd*-I and *bd*-II oxidases. *Sci. Rep.* **2021**, *11*, 23852. [CrossRef]
128. Miyoshi, H.; Takegami, K.; Sakamoto, K.; Mogi, T.; Iwamura, H. Characterization of the ubiquinol oxidation sites in cytochromes *bo* and *bd* from *Escherichia coli* using aurachin C analogues. *J. Biochem.* **1999**, *125*, 138–142. [CrossRef]
129. Makarchuk, I.; Nikolaev, A.; Thesseling, A.; Dejon, L.; Lamberty, D.; Stief, L.; Speicher, A.; Friedrich, T.; Hellwig, P.; Nasiri, H.R.; et al. Identification and optimization of quinolone-based inhibitors against cytochrome bd oxidase using an electrochemical assay. *Electrochim. Acta* **2021**, *381*, 138293. [CrossRef]
130. Lu, P.; Heineke, M.H.; Koul, A.; Andries, K.; Cook, G.M.; Lill, H.; van Spanning, R.; Bald, D. The cytochrome *bd*-type quinol oxidase is important for survival of *Mycobacterium smegmatis* under peroxide and antibiotic-induced stress. *Sci. Rep.* **2015**, *5*, 10333. [CrossRef]
131. Harikishore, A.; Chong, S.S.M.; Ragunathan, P.; Bates, R.W.; Gruber, G. Targeting the menaquinol binding loop of mycobacterial cytochrome *bd* oxidase. *Mol. Divers.* **2021**, *25*, 517–524. [CrossRef]
132. Hopfner, S.M.; Lee, B.S.; Kalia, N.P.; Miller, M.J.; Pethe, K.; Moraski, G.C. Structure guided generation of thieno[3,2-d]pyrimidin-4-amine *Mycobacterium tuberculosis bd* oxidase inhibitors. *RSC Med. Chem.* **2021**, *12*, 73–77. [CrossRef] [PubMed]
133. Anand, P.; Akhter, Y. A review on enzyme complexes of electron transport chain from *Mycobacterium tuberculosis* as promising drug targets. *Int. J. Biol. Macromol.* **2022**, *212*, 474–494. [CrossRef] [PubMed]
134. Hards, K.; Cheung, C.Y.; Waller, N.; Adolph, C.; Keighley, L.; Tee, Z.S.; Harold, L.K.; Menorca, A.; Bujaroski, R.S.; Buckley, B.J.; et al. An amiloride derivative is active against the F_1F_o-ATP synthase and cytochrome *bd* oxidase of *Mycobacterium tuberculosis*. *Commun. Biol.* **2022**, *5*, 166. [CrossRef]

135. Arjona, D.; Wikstrom, M.; Adelroth, P. Nitric oxide is a potent inhibitor of the *cbb*3-type heme-copper oxidases. *FEBS Lett.* **2015**, *589*, 1214–1218. [CrossRef] [PubMed]
136. Brown, G.C.; Cooper, C.E. Nanomolar concentrations of nitric oxide reversibly inhibit synaptosomal respiration by competing with oxygen at cytochrome oxidase. *FEBS Lett.* **1994**, *356*, 295–298. [CrossRef]
137. Cooper, C.E.; Davies, N.A.; Psychoulis, M.; Canevari, L.; Bates, T.E.; Dobbie, M.S.; Casley, C.S.; Sharpe, M.A. Nitric oxide and peroxynitrite cause irreversible increases in the K_m for oxygen of mitochondrial cytochrome oxidase: In Vitro and In Vivo studies. *Biochim. Biophys. Acta* **2003**, *1607*, 27–34. [CrossRef]
138. Torres, J.; Cooper, C.E.; Wilson, M.T. A common mechanism for the interaction of nitric oxide with the oxidized binuclear centre and oxygen intermediates of cytochrome *c* oxidase. *J. Biol. Chem.* **1998**, *273*, 8756–8766. [CrossRef]
139. Mason, M.G.; Nicholls, P.; Wilson, M.T.; Cooper, C.E. Nitric oxide inhibition of respiration involves both competitive (heme) and noncompetitive (copper) binding to cytochrome *c* oxidase. *Proc. Natl. Acad. Sci. USA* **2006**, *103*, 708–713. [CrossRef]
140. Sarti, P.; Forte, E.; Mastronicola, D.; Giuffre, A.; Arese, M. Cytochrome *c* oxidase and nitric oxide in action: Molecular mechanisms and pathophysiological implications. *Biochim. Biophys. Acta* **2012**, *1817*, 610–619. [CrossRef]
141. Chen, J.; Xie, P.; Huang, Y.; Gao, H. Complex interplay of heme-copper oxidases with nitrite and nitric oxide. *Int. J. Mol. Sci.* **2022**, *23*, 979. [CrossRef]
142. Borisov, V.B.; Forte, E.; Konstantinov, A.A.; Poole, R.K.; Sarti, P.; Giuffre, A. Interaction of the bacterial terminal oxidase cytochrome *bd* with nitric oxide. *FEBS Lett.* **2004**, *576*, 201–204. [CrossRef] [PubMed]
143. Borisov, V.B.; Forte, E.; Sarti, P.; Brunori, M.; Konstantinov, A.A.; Giuffre, A. Redox control of fast ligand dissociation from *Escherichia coli* cytochrome *bd*. *Biochem. Biophys. Res. Commun.* **2007**, *355*, 97–102. [CrossRef] [PubMed]
144. Carabet, L.A.; Guertin, M.; Lague, P.; Lamoureux, G. Mechanism of the nitric oxide dioxygenase reaction of *Mycobacterium tuberculosis* hemoglobin N. *J. Phys. Chem. B* **2017**, *121*, 8706–8718. [CrossRef] [PubMed]
145. Giuffre, A.; Stubauer, G.; Sarti, P.; Brunori, M.; Zumft, W.G.; Buse, G.; Soulimane, T. The heme-copper oxidases of *Thermus thermophilus* catalyze the reduction of nitric oxide: Evolutionary implications. *Proc. Natl. Acad. Sci. USA* **1999**, *96*, 14718–14723. [CrossRef]
146. Butler, C.; Forte, E.; Maria Scandurra, F.; Arese, M.; Giuffre, A.; Greenwood, C.; Sarti, P. Cytochrome bo_3 from *Escherichia coli*: The binding and turnover of nitric oxide. *Biochem. Biophys. Res. Commun.* **2002**, *296*, 1272–1278. [CrossRef]
147. Forte, E.; Urbani, A.; Saraste, M.; Sarti, P.; Brunori, M.; Giuffre, A. The cytochrome cbb_3 from *Pseudomonas stutzeri* displays nitric oxide reductase activity. *Eur. J. Biochem.* **2001**, *268*, 6486–6491. [CrossRef]
148. Huang, Y.; Reimann, J.; Lepp, H.; Drici, N.; Adelroth, P. Vectorial proton transfer coupled to reduction of O_2 and NO by a heme-copper oxidase. *Proc. Natl. Acad. Sci. USA* **2008**, *105*, 20257–20262. [CrossRef]
149. Stubauer, G.; Giuffre, A.; Brunori, M.; Sarti, P. Cytochrome *c* oxidase does not catalyze the anaerobic reduction of NO. *Biochem. Biophys. Res. Commun.* **1998**, *245*, 459–465. [CrossRef]
150. Ohta, T.; Soulimane, T.; Kitagawa, T.; Varotsis, C. Nitric oxide activation by caa_3 oxidoreductase from *Thermus thermophilus*. *Phys. Chem. Chem. Phys.* **2015**, *17*, 10894–10898. [CrossRef]
151. Blomberg, M.R.A. Activation of O_2 and NO in heme-copper oxidases-mechanistic insights from computational modelling. *Chem. Soc. Rev.* **2020**, *49*, 7301–7330. [CrossRef]
152. Jones-Carson, J.; Husain, M.; Liu, L.; Orlicky, D.J.; Vazquez-Torres, A. Cytochrome *bd*-dependent bioenergetics and antinitrosative defenses in *Salmonella* pathogenesis. *mBio* **2016**, *7*, e02052-02016. [CrossRef] [PubMed]
153. Shepherd, M.; Achard, M.E.; Idris, A.; Totsika, M.; Phan, M.D.; Peters, K.M.; Sarkar, S.; Ribeiro, C.A.; Holyoake, L.V.; Ladakis, D.; et al. The cytochrome *bd*-I respiratory oxidase augments survival of multidrug-resistant *Escherichia coli* during infection. *Sci. Rep.* **2016**, *6*, 35285. [CrossRef] [PubMed]
154. Beebout, C.J.; Eberly, A.R.; Werby, S.H.; Reasoner, S.A.; Brannon, J.R.; De, S.; Fitzgerald, M.J.; Huggins, M.M.; Clayton, D.B.; Cegelski, L.; et al. Respiratory heterogeneity shapes biofilm formation and host colonization in uropathogenic *Escherichia coli*. *mBio* **2019**, *10*, e02400-18. [CrossRef] [PubMed]
155. Mason, M.G.; Shepherd, M.; Nicholls, P.; Dobbin, P.S.; Dodsworth, K.S.; Poole, R.K.; Cooper, C.E. Cytochrome *bd* confers nitric oxide resistance to *Escherichia coli*. *Nat. Chem. Biol.* **2009**, *5*, 94–96. [CrossRef] [PubMed]
156. Meng, Q.; Yin, J.; Jin, M.; Gao, H. Distinct nitrite and nitric oxide physiologies in *Escherichia coli* and *Shewanella oneidensis*. *Appl. Environ. Microbiol.* **2018**, *84*, e00559-00518. [CrossRef] [PubMed]
157. Pullan, S.T.; Gidley, M.D.; Jones, R.A.; Barrett, J.; Stevanin, T.M.; Read, R.C.; Green, J.; Poole, R.K. Nitric oxide in chemostat-cultured *Escherichia coli* is sensed by Fnr and other global regulators: Unaltered methionine biosynthesis indicates lack of S nitrosation. *J. Bacteriol.* **2007**, *189*, 1845–1855. [CrossRef]
158. Hyduke, D.R.; Jarboe, L.R.; Tran, L.M.; Chou, K.J.; Liao, J.C. Integrated network analysis identifies nitric oxide response networks and dihydroxyacid dehydratase as a crucial target in *Escherichia coli*. *Proc. Natl. Acad. Sci. USA* **2007**, *104*, 8484–8489. [CrossRef]
159. Richardson, A.R.; Dunman, P.M.; Fang, F.C. The nitrosative stress response of *Staphylococcus aureus* is required for resistance to innate immunity. *Mol. Microbiol.* **2006**, *61*, 927–939. [CrossRef]
160. Moore, C.M.; Nakano, M.M.; Wang, T.; Ye, R.W.; Helmann, J.D. Response of *Bacillus subtilis* to nitric oxide and the nitrosating agent sodium nitroprusside. *J. Bacteriol.* **2004**, *186*, 4655–4664. [CrossRef]

161. Shi, L.; Sohaskey, C.D.; Kana, B.D.; Dawes, S.; North, R.J.; Mizrahi, V.; Gennaro, M.L. Changes in energy metabolism of *Mycobacterium tuberculosis* in mouse lung and under In Vitro conditions affecting aerobic respiration. *Proc. Natl. Acad. Sci. USA* **2005**, *102*, 15629–15634. [CrossRef]
162. Cai, Y.; Jaecklein, E.; Mackenzie, J.S.; Papavinasasundaram, K.; Olive, A.J.; Chen, X.; Steyn, A.J.C.; Sassetti, C.M. Host immunity increases *Mycobacterium tuberculosis* reliance on cytochrome *bd* oxidase. *PLoS Pathog.* **2021**, *17*, e1008911. [CrossRef] [PubMed]
163. Stevanin, T.M.; Ioannidis, N.; Mills, C.E.; Kim, S.O.; Hughes, M.N.; Poole, R.K. Flavohemoglobin Hmp affords inducible protection for *Escherichia coli* respiration, catalyzed by cytochromes *bo'* or *bd*, from nitric oxide. *J. Biol. Chem.* **2000**, *275*, 35868–35875. [CrossRef] [PubMed]
164. Sarti, P.; Giuffre, A.; Forte, E.; Mastronicola, D.; Barone, M.C.; Brunori, M. Nitric oxide and cytochrome *c* oxidase: Mechanisms of inhibition and NO degradation. *Biochem. Biophys. Res. Commun.* **2000**, *274*, 183–187. [CrossRef] [PubMed]
165. Borisov, V.B.; Forte, E.; Sarti, P.; Brunori, M.; Konstantinov, A.A.; Giuffre, A. Nitric oxide reacts with the ferryl-oxo catalytic intermediate of the Cu_B-lacking cytochrome *bd* terminal oxidase. *FEBS Lett.* **2006**, *580*, 4823–4826. [CrossRef] [PubMed]
166. Borisov, V.B.; Forte, E.; Giuffre, A.; Konstantinov, A.; Sarti, P. Reaction of nitric oxide with the oxidized di-heme and heme-copper oxygen-reducing centers of terminal oxidases: Different reaction pathways and end-products. *J. Inorg. Biochem.* **2009**, *103*, 1185–1187. [CrossRef]
167. Giuffre, A.; Barone, M.C.; Mastronicola, D.; D'Itri, E.; Sarti, P.; Brunori, M. Reaction of nitric oxide with the turnover intermediates of cytochrome *c* oxidase: Reaction pathway and functional effects. *Biochemistry* **2000**, *39*, 15446–15453. [CrossRef]
168. Yang, K.; Borisov, V.B.; Konstantinov, A.A.; Gennis, R.B. The fully oxidized form of the cytochrome *bd* quinol oxidase from *E. coli* does not participate in the catalytic cycle: Direct evidence from rapid kinetics studies. *FEBS Lett.* **2008**, *582*, 3705–3709. [CrossRef]
169. Borisov, V.B.; Forte, E.; Siletsky, S.A.; Sarti, P.; Giuffre, A. Cytochrome *bd* from *Escherichia coli* catalyzes peroxynitrite decomposition. *Biochim. Biophys. Acta* **2015**, *1847*, 182–188. [CrossRef]
170. Sharpe, M.A.; Cooper, C.E. Interaction of peroxynitrite with mitochondrial cytochrome oxidase. Catalytic production of nitric oxide and irreversible inhibition of enzyme activity. *J. Biol. Chem.* **1998**, *273*, 30961–30972. [CrossRef]
171. Floris, R.; Piersma, S.R.; Yang, G.; Jones, P.; Wever, R. Interaction of myeloperoxidase with peroxynitrite. A comparison with lactoperoxidase, horseradish peroxidase and catalase. *Eur. J. Biochem.* **1993**, *215*, 767–775. [CrossRef]
172. Van Zyl, J.M.; Van der Walt, B.J. Apparent hydroxyl radical generation without transition metal catalysis and tyrosine nitration during oxidation of the anti-tubercular drug, isonicotinic acid hydrazide. *Biochem. Pharmacol.* **1994**, *48*, 2033–2042. [CrossRef]
173. Stern, M.K.; Jensen, M.P.; Kramer, K. Peroxynitrite decomposition catalysts. *J. Am. Chem. Soc.* **1996**, *118*, 8735–8736. [CrossRef]
174. Bryk, R.; Griffin, P.; Nathan, C. Peroxynitrite reductase activity of bacterial peroxiredoxins. *Nature* **2000**, *407*, 211–215. [CrossRef] [PubMed]
175. Ferrer-Sueta, G.; Campolo, N.; Trujillo, M.; Bartesaghi, S.; Carballal, S.; Romero, N.; Alvarez, B.; Radi, R. Biochemistry of peroxynitrite and protein tyrosine nitration. *Chem. Rev.* **2018**, *118*, 1338–1408. [CrossRef] [PubMed]